Research Square

Preprints are preliminary reports that have not undergone peer review.
They should not be considered conclusive, used to inform clinical practice,
or referenced by the media as validated information.

Mechanism of Organic Plant Protection Technology in Controlling Apple Bitter Pit: Insights from Integrated Transcriptomic and Metabolomic Analyses

Zhu Li
20240003@ztu.edu.cn

Zhaotong University
Shikui Wang
Beijing Union University
Rongjing Cai
Zhaotong University
Yingchun Huang
Beijing Union University
Bin Xia
Beijing Union University
Ling Mao
Zhaotong University
Yanfei Song
Zhaotong University
Tingmen Jiao
Zhaotong University
Jiansong Qi
Zhaotong University
Yue Chen
Zhaotong University

Research Article

Keywords: Apple Bitter Pit, Organic Plant Protection Technology (OPPT), Malus domestica 'Qincui', Flavonoid biosynthesis, Calcium metabolism

Posted Date: September 29th, 2026

DOI: https://doi.org/10.21203/rs.3.rs-11042718/v1

License: This work is licensed under a Creative Commons Attribution 4.0 International License. Read Full License

Additional Declarations: No competing interests reported.

Abstract

Apple bitter pit (ABP), a severe physiological disorder, severely impairs the quality and yield of the susceptible 'Qincui' apple. This study investigated the control efficacy and mechanism of a three-in-one Organic Plant Protection Technology (OPPT) against ABP, with treatments set as control (CK), untreated diseased (UD), and OPPT-sprayed healthy groups. Results showed OPPT significantly reduced ABP incidence to 14.84%, improved fruit quality, enhanced antioxidant defense systems, mitigated oxidative damage, repaired fruit cell structural damage, and restored fruit calcium levels to the healthy level. Integrated transcriptomic and metabolomic analyses revealed OPPT reshaped fruit gene and metabolite profiles, with the flavonoid biosynthesis pathway as the core regulatory node, upregulating key genes (CHS, FLS, etc.) and promoting flavonoid metabolite accumulation. In conclusion, OPPT controls ABP via multi-dimensional regulation of phenotype, physiology, cell structure and molecular metabolism, providing a novel green strategy for managing physiological disorders in apple fruit, preserving fruit quality and nutritional value, and supporting the sustainable production of high-quality fresh horticultural foods.

1. Introduction

Apple (*Malus domestica* Borkh.) is one of the most widely cultivated commercial fruit tree species worldwide. With its rich nutritional profile, unique flavor, and excellent storage tolerance, it occupies a pivotal position in the global fruit market[1–3]t. However, the large-scale and intensive development of the apple industry is challenged by multiple diseases. Among them, Apple Bitter Pit (ABP), a typical physiological disorder, has become one of the key limiting factors for apple quality and yield[4]. ABP mainly occurs during fruit ripening and storage, manifesting as sunken brown lesions on the epidermis and bitter flesh, which severely reduce fruit quality and edible value[4–6] With the increasing consumer demand for high-quality apples, the effective control of ABP has become an urgent issue to be addressed in the global apple industry.

Zhaotong City in Yunnan Province, China, is a high-quality apple production base in southern China. Its unique ecological and climatic conditions have nurtured characteristic apple varieties with the traits of "early maturity, sweetness, crispness, aroma, and bright color". Among them, the 'Qincui' apple, a widely cultivated new mid-late maturing variety introduced from Northwest A&F University, was bred from the cross between 'Changfu 2' and 'Honeycrisp'. This apple variety is popular among consumers for its thin peel, crisp flesh, abundant juice, sweet taste, and bright color. Unfortunately, after years of cultivation and observation, we found that this variety is highly susceptible to bitter pit, with complex and diverse causative factors. At present, the occurrence mechanism of bitter pit is widely considered to be related to multiple factors, including calcium metabolism imbalance, mineral nutrient disorder, physiological disturbance during fruit development and senescence, and cell wall structural changes[7–10]. Meanwhile, it is regulated by multiple factors such as variety, rootstock, cultivation management, and storage conditions[5, 11, 12]. Although various control measures have been attempted in production, including calcium fertilization and chemical agent treatment, they generally suffer from high cost, poor environmental adaptability, high risk of environmental pollution, and unstable control efficacy, failing to fundamentally solve the damage caused by bitter pit[13–15]. Therefore, the development of environmentally friendly, low-cost, efficient, and stable green control technologies for apple bitter pit, along with the systematic elucidation of their underlying mechanisms, has become an urgent requirement for the sustainable development of the apple industry.

In response to this challenge, green plant protection technologies have gradually become a research hotspot in agricultural disease control due to their advantages of strong environmental compatibility, low residue, and sustainability. The three-in-one Organic Plant Protection Technology (OPPT) introduced in this study is compounded with 20% stress-resistant nano ecological film, 5% carvacrol, and 0.5% chitosan, each with well-defined biological activities. The stress-resistant nano ecological film has multiple functions including disease prevention, pest control, sunscald prevention, calcium supplementation, and immunity enhancement[16]. As a plant-derived agent, carvacrol has the characteristics of broad-spectrum antibacterial activity, yield and quality improvement, environmental friendliness, and no induction of drug resistance, making it an optimal choice for green fruit production[17–19]. Chitosan can inhibit the propagation of pathogenic bacteria, induce plant immune responses, and promote crop growth[20–23]. With the advantages of multi-component, multi-target, and multi-effect properties, OPPT matches the multi-factorial and multi-mechanism occurrence characteristics of apple bitter pit, thus holding great potential as an effective new technology for the green control of this disorder. Previous studies have shown that this OPPT exhibits excellent performance in the control of apple diseases and pests such as early defoliation disease and Tetranychus urticae. It not only significantly reduces the incidence of pests and diseases, but also promotes the growth of fruits and leaves, improves fruit quality, and has a pesticide residue level far lower than that of chemical control technologies, providing an effective way for green fruit production[24, 25]However, there are no relevant research reports on the control efficacy and molecular mechanism of this technology against apple bitter pit to date.

Based on this, this study took the highly susceptible 'Qincui' apple in Zhaotong, Yunnan as the research object, to systematically explore the molecular mechanism of OPPT in controlling apple bitter pit. First, we clarified the control efficacy of OPPT by analyzing its effect on the incidence of bitter pit in apples at harvest. On this basis, we further investigated the changes in fruit quality, reactive oxygen species (ROS) metabolism system, cytological structure, and calcium distribution in fruits after OPPT treatment, to clarify its quality improvement effect and regulatory effect at the physiological level. Subsequently, through integrated metabolomic and transcriptomic analysis, we constructed a synergistic interaction network of "genes-metabolites", and mined the key genes and core metabolic pathways involved in the control of apple bitter pit by OPPT. Finally, we elucidated the core mechanism of OPPT in controlling apple bitter pit from a multi-dimensional perspective of "phenotype-physiology-metabolism-gene". This study not only fills the research gap in the molecular mechanism of OPPT against apple bitter pit and provides a solid theoretical support for the optimization

and promotion of this technology, but also takes this as a breakthrough to provide a new paradigm for the green control of apple physiological disorders, thereby promoting the sustainable development of the global apple industry.

2. Materials and Methods

2.1 Experimental Materials and Design

The experimental materials were 5-year-old 'Qincui' apple trees, planted in the State Farms Apple Demonstration Base and farmers' orchards in Haibian Village, Yongfeng Town, Zhaoyang District (103.42° E, 27.19° N), Zhaotong City, Yunnan Province, with a wide-row and narrow-plant trellis high-density cultivation system (plant spacing × row spacing: 1.5 m × 4 m, planting density: 192 plants/hm²). Prior to the experiment, formal permission was obtained from the orchard owners and farm management for conducting the field trial and fruit sampling on the site. The OPPT mixture was composed of 20% stress-resistant nano ecological film (Micro-Iodine Technology Co., Ltd., China), 5% carvacrol (Micro-Iodine Technology Co., Ltd., China), and 0.5% chitosan (Micro-Iodine Technology Co., Ltd., China). The experiment set up three groups: CK (sprayed with equal volume of clean water, healthy fruits), UD (sprayed with equal volume of clean water, naturally diseased fruits), and OPPT (sprayed with OPPT mixture, healthy fruits). The OPPT group was sprayed once at the beginning of each month from April to September, for a total of 6 times, using a motorized sprayer to ensure full wetting of fruits and leaves. The control groups were sprayed with equal volume of clean water, and other cultivation management measures (fertilization, irrigation, pruning, etc.) were kept consistent.

2.2 Incidence Statistics

The five-point sampling method was adopted, and 10 fruit trees with consistent growth were selected in the east, south, west, north, and center of the orchard, respectively. The fruit phenotype was observed at harvest, and the incidence rate was calculated with the formula: Incidence rate (%) = (number of diseased fruits / total number of sampled fruits) × 100%. 300 fruits were sampled for each group.

2.3 Determination of Fruit Quality

36 homogeneous fruits (12 per replicate) were randomly selected from each group to determine the following indicators: single fruit weight, fruit shape index (longitudinal diameter / transverse diameter), soluble solids content (hand-held refractometer, DL339101, Deli, China), fruit firmness and crispness (texture analyzer, CTX, Brookfield); soluble sugar content (G0501W, Geruisi-Bio, anthrone colorimetric method at 620 nm); titratable acid content (G0174D, Geruisi-Bio, acid-base neutralization titration method); vitamin C (Vc) content (G0201W, Geruisi-Bio, iron reduction colorimetric method at 534 nm); total flavonoid content (G0201W, Geruisi-Bio, iron reduction colorimetric method at 534 nm); total phenol content (G0117F, Geruisi-Bio, Folin-Ciocalteu method at 760 nm). Apple fruit samples were accurately weighed, and the quantitative detection of titratable acid, vitamin C, total flavonoids, and total phenols was performed according to the instructions of the detection kits (Suzhou Geruisi Biotechnology Co., Ltd., Suzhou, China).

2.4 Determination of Oxidative Damage and Antioxidant Enzyme Activity Indicators

Apple fruit samples were accurately weighed to determine oxidative damage indicators: malondialdehyde (MDA) content (G0109W, Geruisi-Bio, TBA reaction method at 532 nm), hydrogen peroxide (H_2O_2) content (G0168W, Geruisi-Bio, colorimetric method at 510 nm), superoxide anion (O_2^-) production rate (G0116W, Geruisi-Bio, hydroxylamine reaction method at 540 nm). Antioxidant enzyme activity indicators were also determined: superoxide dismutase (SOD) activity (G0103W, Geruisi-Bio, NBT photochemical reduction method at 560 nm), catalase (CAT) activity (G0105W, Geruisi-Bio, H_2O_2 catalytic color development method at 510 nm), ascorbate peroxidase (APX) activity (G0203W, Geruisi-Bio, ascorbic acid oxidation method at 290 nm), peroxidase (POD) activity (G0107W, Geruisi-Bio, H_2O_2-guaiacol method at 470 nm), and 1,1-Diphenyl-2-picrylhydrazyl radical (DPPH) scavenging capacity (G0128W, Geruisi-Bio, DPPH colorimetric method at 517 nm). All quantitative detections were performed according to the instructions of the detection kits (Suzhou Geruisi Biotechnology Co., Ltd., Suzhou, China).

2.5 Safranin O-Fast Green Staining

Safranin O-Fast Green staining was performed according to the protocol described in our previous study[26] with slight modifications. Briefly, apple fruit tissue blocks of 1 cm × 0.5 cm × 0.1 cm (length × width × thickness) were cut and placed into 20 volumes of FAA fixative solution (90 mL 70% ethanol + 5 mL glacial acetic acid + 5 mL formalin), and fixed at room temperature for 24 h. Subsequently, the samples were dehydrated in a gradient ethanol series of 70%, 80%, 90%, 95%, and absolute ethanol, then immersed in a mixture of absolute ethanol / xylene for 1.5 h, and cleared in xylene for 3 times (1.5 h each). The samples were immersed in a paraffin / toluene mixture at 55℃ for 6–8 h, then in 100% paraffin at 65℃ for 13–15 h, followed by embedding. The wax blocks were trimmed and sectioned on a rotary microtome, and dried in an electric thermostatic drying oven at 50℃. For staining, the sections were first dewaxed in environment-friendly dewaxing and clearing solution Ⅰ and Ⅱ for 20 min each, then rehydrated in a gradient series of absolute ethanol Ⅰ, Ⅱ, and 75% ethanol for 5 min each, followed by rinsing with tap water. The sections were then stained in safranin staining solution for 2 min, excess dye was quickly washed off with tap water, and the sections were decolorized in gradient ethanol of 50%, 70%, and 80% for 3–8 s each. Afterwards, the sections were stained in fast green staining solution for 6–20 s, and dehydrated sequentially in three cylinders of absolute ethanol for 5 s, 10 s, and 20 s, respectively. Finally, the sections were cleared in xylene for 5 min, mounted with neutral balsam, examined and imaged under an optical microscope.

2.6 Transmission Electron Microscopy

Transmission electron microscopy observation was performed according to the protocol described in our previous study[26]with slight modifications. Briefly, apple fruit tissue blocks of 1 mm^3 were cut and immediately placed into electron microscope fixative solution. Air was extracted with a vacuum pump until the tissue blocks sank to the bottom, and the samples were fixed at room temperature for 2 h, then transferred to 4℃ for storage in the dark. The samples were rinsed 3 times with 0.1 M phosphate buffer (pH 7.4) for 15 min each, then post-fixed with 1% osmium tetroxide prepared in 0.1 M phosphate buffer for 7 h at room temperature in the dark, followed by repeating the rinsing procedure. The samples were dehydrated sequentially in 30%, 50%, 70%, 80%, 90%, 95%, and 100% ethanol for 1 h each, then treated in mixtures of absolute ethanol and acetone at ratios of 3:1, 1:1, and 1:3 for 0.5 h each, and finally dehydrated in pure acetone for 1 h. At 37℃, the samples were first treated in a 3:1 mixture of acetone and 812 embedding medium for 2–4 h, then infiltrated overnight in a 1:1 mixture, followed by treatment in a 1:3 mixture for 2–4 h, and finally in pure 812 embedding medium for 5–8 h. The samples were inserted into embedding plates containing pure embedding medium, left overnight at 37℃, and polymerized in an oven at 60℃ for 48 h. Ultrathin sections of 60–80 nm were prepared with an ultramicrotome, and collected on 150-mesh formvar-coated copper grids. The sections were stained with 2% uranyl acetate saturated alcohol solution for 8 min in the dark, washed 3 times with 70% ethanol and ultrapure water each, then stained with 2.6% lead citrate solution for 8 min in a CO_2-free environment, washed 3 times with ultrapure water, and dried overnight at room temperature. After sample preparation, the sections were observed and imaged under a transmission electron microscope.

2.7 Scanning Electron Microscopy with Energy Dispersive Spectroscopy (SEM-EDS)

Scanning electron microscopy with energy dispersive spectroscopy (SEM-EDS) was performed according to the protocol described in previous studies[27, 28]with slight modifications. Briefly, fresh apple fruit tissues were first sampled accurately within 1–3 min, with the tissue block area not exceeding 3 mm^2. The samples were rinsed with PBS to remove surface impurities, quickly placed into electron microscope fixative solution and fixed at room temperature for 2 h, then transferred to 4℃ for storage. Subsequently, the samples were rinsed 3 times with 0.1 M phosphate buffer (pH 7.4) for 15 min each, post-fixed with 1% osmium tetroxide for 1–2 h at room temperature in the dark, then dehydrated sequentially in a gradient series of 30%, 50%, 70%, 80%, 90%, 95%, 100%, and 100% absolute ethanol for 15 min each, and treated with isoamyl acetate for 15 min. Afterwards, the samples were dried with a critical point dryer (K850, Quorum), and finally coated with gold for about 30 s using an ion sputtering coater (MC1000, Hitachi) to complete the conductive treatment. The apple fruit samples were imaged under a scanning electron microscope (SU8100, Hitachi), with an adapted accelerating voltage to clearly present the microstructure of fruit tissues and the characteristics of the target analysis area. The elemental composition was determined using an X-ray energy dispersive spectrometer (EDS, ULTIMMAX 100, Oxford) with a mapping scan mode. To ensure accurate quantification of elemental peaks, the EDS system was calibrated with standard reference materials. Briefly, for mapping scan analysis, the target tissue area of the apple fruit was selected as the detection range. By collecting characteristic X-ray photons in this area, a mapping distribution map of each element was generated (different elements were marked with exclusive colors to intuitively present the spatial distribution characteristics). Subsequently, AZtech software was used to process and analyze the acquired SEM images and EDS mapping scan spectral data.

2.8 Transcriptomic Analysis

Apple fruit samples were selected, with three biological replicates set for each group for transcriptome sequencing analysis. Transcriptome sequencing was performed on the Illumina platform by Novogene Bioinformatics Technology Co., Ltd. (Tianjin, China). Briefly, a strand-specific library construction method was adopted. mRNA was enriched from total RNA using Oligo dT magnetic beads, fragmented, and then reverse-transcribed into first-strand cDNA using random hexamer primers. Second-strand cDNA was synthesized with dUTP instead of dTTP. Subsequently, library construction was completed through end repair, A-tailing, adapter ligation, fragment selection, amplification, and purification. The library was quantified by Qubit fluorometer and real-time fluorescent quantitative PCR, and the fragment size distribution was verified with a bioanalyzer. After qualification, the library was sequenced on the Illumina platform using sequencing-by-synthesis technology. Raw data were processed with fastp software to remove reads containing adapters, ploy-N, and low-quality reads to obtain clean reads, and the Q20, Q30, and GC content were calculated. Clean reads were aligned to the apple reference genome using HISAT2 software, new transcripts were predicted with StringTie, and gene counts were calculated with featureCounts and converted to FPKM values for the quantification of expression levels. Differential expression analysis was performed using the DESeq2 R package, with padj ≤ 0.05 and $|\log_2(\text{fold change})| \geq 1$ as the threshold for significant differential expression. Subsequent bioinformatics analysis was performed using software such as clusterProfiler. The reference genome (https://ftp.ncbi.nlm.nih.gov/genomes/all/GCA/004/115/385/GCA_004115385.1_ASM411538v1/GCA_004115385.1_ASM411538v1_genomic.fna.gz) and corresponding annotation file (https://ftp.ncbi.nlm.nih.gov/genomes/all/GCA/004/115/385/GCA_004115385.1_ASM411538v1/GCA_004115385.1_ASM411538v1_genomic.gff.gz) were used for analysis.

2.9 Metabolomic Analysis

Apple fruit samples were selected for untargeted metabolomic analysis, with five biological replicates set for each group. Meanwhile, QC samples (equal volume mixture of each experimental sample) and blank samples (53% methanol aqueous solution) were prepared to monitor the stability of the experiment and remove background interference, respectively. Untargeted metabolomic analysis was performed by Novogene Bioinformatics Technology Co., Ltd. (Tianjin, China). Briefly, 100 mg of apple fruit tissue ground in liquid nitrogen was placed in an EP tube, 500 μL of 80% methanol aqueous solution was added, vortexed, and incubated on ice for 5 min, followed by centrifugation at 15000 g and 4℃ for 20 min. The supernatant was diluted with mass spectrometry-grade water to a methanol content of 53%, and centrifuged again under the same conditions for 20 min. The supernatant was collected for detection. The experiment was performed using Vanquish ultra-high performance liquid chromatography (UHPLC)

coupled with Q Exactive HF/X mass spectrometry. Chromatographic separation was performed on a Hypersil Gold C18 column (100 × 2.1 mm, 1.9 μm) at a column temperature of 40℃, with gradient elution using 0.1% formic acid aqueous solution (phase A) and methanol (phase B) at a flow rate of 0.2 mL/min. Mass spectrometry was performed with an ESI source, and signals were collected in both positive and negative ion modes, with a scanning range of m/z 100–1500. The raw data were converted to mzXML format using ProteoWizard, and peak extraction, alignment, and quantification were completed through XCMS. Metabolites were identified in combination with the KEGG and HMDB databases. After removing background ions with blank samples, data normalization was performed based on QC samples, and compounds with relative peak area CV > 30% in QC were excluded. Finally, multivariate statistical analysis such as PCA and PLS-DA was performed using metaX software. Differential metabolites (DAMs) were screened with the criteria of VIP > 1.0, FC > 1.5 or FC < 0.667, and p-value < 0.05, followed by relevant bioinformatics analysis.

2.10 RT-qPCR Validation

Total RNA was extracted using the CTAB method described in previous studies [29]. Seven differentially expressed genes (DEGs) related to Flavonoid biosynthesis were selected from the apple fruit transcriptome data, and specific primers for reverse transcription-quantitative PCR (RT-qPCR) were designed using SnapGene 8.0 software (**Table S1**). Total RNA was extracted according to the instructions of the TRIzol reagent, and the purity of RNA (A260/A280 between 1.8 and 2.0) was detected by NanoDrop 2000. RNA was reverse-transcribed into complementary DNA (cDNA) using a reverse transcription kit (R312, Vazyme, China). RT-qPCR was performed using ChamQ Universal SYBR qPCR Master Mix (Q711, Vazyme, China) on a CFX96 real-time fluorescence quantitative instrument. The reaction procedure was as follows: pre-denaturation at 95℃ for 30 s; 40 cycles of denaturation at 95℃ for 10 s, annealing and extension at 60℃ for 30 s. The apple EF-1α gene was used as the internal reference[30], and the relative expression level of genes was calculated using the 2^-ΔΔCt method. Three biological replicates and three technical replicates were set for each sample.

2.11 Data Analysis

Statistical analysis was performed using SPSS 25.0 software. One-way analysis of variance (ANOVA) was used to evaluate the effects of different treatments, and Fisher's Least Significant Difference (LSD) test was used for mean comparison, with $p < 0.05$ as the criterion for significant difference. Data were uniformly presented as mean ± standard deviation. Experimental charts were drawn with GraphPad Prism 9, and the layout was optimized with Adobe Illustrator 2023. All experiments were set with at least three independent biological replicates.

3. Results

3.1 Effect of OPPT on the Incidence of Apple Bitter Pit at Harvest

Significant differences in fruit phenotype were observed among different treatment groups. The fruits in the OPPT-treated healthy group had a smooth surface, uniform color, and no typical epidermal depression or brown spots of bitter pit (Fig. 1A). The fruit appearance of the untreated healthy group (CK) and the OPPT-treated healthy group (OPPT) was basically normal, while the fruits in the untreated diseased group (UD) had multiple sunken and brown spots on the surface. The incidence statistics showed that the incidence rate at harvest was approximately 70.99% in the group sprayed with equal volume of clean water, while it was significantly reduced to 14.84% in the group sprayed with equal volume of OPPT (Fig. 1B). This indicated that OPPT significantly reduced the incidence of apple bitter pit at harvest.

3.2 Effect of OPPT on Apple Fruit Quality and Reactive Oxygen Species (ROS) Metabolism System

Significant differences were observed in fruit quality indicators and parameters related to the ROS metabolism system among different treatment groups (Fig. 2). In terms of appearance and basic quality, compared with the CK group, the single fruit weight was significantly reduced in the UD group, while it was significantly increased in the OPPT group compared with the UD group, with no significant difference compared with the CK group. There was no significant difference in fruit shape index among different treatment groups. Compared with the CK group, the fruit firmness and crispness were decreased in the UD group, while they were significantly increased in the OPPT group compared with the UD group, and also higher than those in the CK group to a certain extent (Fig. 2A). In terms of internal nutritional quality, compared with the CK group, the soluble solids content was significantly increased in the UD group, while it was lower in the OPPT group than in the UD group to a certain extent, with no significant difference compared with the CK group. Compared with the CK group, the soluble sugar content was significantly increased in the UD group, while there was no significant difference in the OPPT group compared with the UD group, which was significantly higher than that in the CK group. Compared with the CK group, the titratable acid content was significantly reduced in the UD group, while it was significantly increased in the OPPT group compared with the UD group, with no significant difference compared with the CK group. In terms of non-enzymatic antioxidant substances, compared with the CK group, the Vc content was significantly reduced, while the total flavonoid and total phenol contents were significantly increased in the UD group. The Vc and total flavonoid contents in the OPPT group were significantly higher than those in the other two groups, and the total phenol content was also higher than that in the UD group to a certain extent, which was significantly increased compared with the CK group (Fig. 2A). In terms of differences in the ROS metabolism system, among the oxidative damage indicators, the ROS accumulation and membrane lipid peroxidation were the most severe in the fruits of the UD group, in which the O_2^- production rate, H_2O_2 content, and MDA content were significantly increased compared with the CK group. The OPPT treatment reversed this trend, although there were still differences between the OPPT group and the CK group (Fig. 2B). In terms of antioxidant enzyme activity and overall antioxidant capacity, compared with the CK group, the antioxidant enzyme

system was significantly inhibited in the fruits of the UD group, with significantly reduced SOD activity, CAT activity, POD activity, APX activity, and DPPH free radical scavenging capacity. The OPPT treatment reversed this trend, although there were still differences between the OPPT group and the CK group (Fig. 2B). These results indicated that OPPT may reduce the risk of bitter pit occurrence by improving fruit nutritional quality, strengthening the non-enzymatic and enzymatic antioxidant defense systems, and reducing ROS accumulation and oxidative damage.

3.3 Effect of OPPT on Cytology and Calcium Element in Apple Fruits

The results of Safranin O-Fast Green staining showed that the fruit cells in the CK group maintained a relatively complete cell morphology with orderly arrangement, while the fruit cells in the UD group were loosely and disorderly arranged with structural rupture. The fruit cells in the OPPT group were closely and neatly arranged (Fig. 3A). Meanwhile, the ultrastructure of the pulp in each group was observed by transmission electron microscopy. The results showed that the organelles in the CK group and OPPT group had normal morphology and stable cell size, with intact organelles such as chloroplasts, mitochondria, Golgi apparatus, and endoplasmic reticulum visible, and the mitochondria had complete cristae structure. The number of organelles in the UD group was significantly reduced, and the morphology of organelles such as chloroplasts, mitochondria, and endoplasmic reticulum was altered (Fig. 3B). The results of scanning electron microscopy with energy dispersive spectroscopy (SEM-EDS) showed that the Ca content was significantly reduced in the UD group compared with the CK group, while it was significantly increased in the OPPT group compared with the UD group, with no significant difference compared with the CK group (Fig. 3C).

3.4 Comparative Analysis of Apple Fruit Transcriptome

To reveal the molecular mechanism of OPPT regulating the resistance of apple to bitter pit, transcriptome sequencing analysis was performed on apple fruits from the CK group, UD group, and OPPT group. The quality assessment of sequencing data showed that after data filtering, an average of approximately 49.32 million, 51.52 million, and 47.19 million clean reads were obtained for the three biological replicates of each group, respectively, with Q30 higher than 96.55% and an average GC content of 47.15% **(Table S2)**, indicating excellent sequencing data quality and high base accuracy. Clean reads were aligned to the apple reference genome, with an average mapping rate of 92.01% and a unique mapping rate of more than 88.37% **(Table S3)**, indicating a high matching degree between the sequencing data and the reference genome, which could be used for subsequent differentially expressed gene (DEG) analysis. The sample correlation analysis showed that the correlation coefficient (R^2) between different biological replicates within the same treatment group was higher than 0.95; while the correlation between different treatment groups was significantly lower than that within groups, especially the lowest correlation between the CK group and the UD group (Fig. 4A), indicating significant differences in gene expression patterns among the three groups of samples, and reliable experimental stability within groups. Principal component analysis (PCA) further verified the differences between groups. Samples from the CK group, UD group, and OPPT group were clustered in different regions, with tight clustering of samples within groups and clear boundaries between groups. The first principal component (PC1) explained 43.53% of the expression variation, and the second principal component (PC2) explained 35.49% of the variation, with a cumulative variance contribution rate of 79.02%, which could effectively distinguish the gene expression differences among the three groups of samples (Fig. 4B). DEGs were identified with the screening criteria of padj ≤ 0.05 and $|\log_2(\text{fold change})| \geq 1$. Venn diagram analysis showed that there were 395 common DEGs among the three comparisons. There were 1162 common DEGs between the UD vs CK group and the OPPT vs UD group, 1341 common DEGs between the UD vs CK group and the OPPT vs CK group, and 1047 common DEGs between the OPPT vs UD group and the OPPT vs CK group. There were 649 unique DEGs in the UD vs CK group, 615 unique DEGs in the OPPT vs UD group, and 750 unique DEGs in the OPPT vs CK group (Fig. 4C). The bar chart quantified the upregulated and downregulated DEGs in pairwise comparisons among the three groups of samples. A total of 2757 DEGs were identified in the UD vs CK group, including 1185 upregulated DEGs and 1572 downregulated DEGs. A total of 2425 DEGs were identified in the OPPT vs UD group, including 762 upregulated DEGs and 1663 downregulated DEGs. A total of 2739 DEGs were identified in the OPPT vs CK group, including 738 upregulated DEGs and 2001 downregulated DEGs (Fig. 4D) **(Tables S4-S6)**.

To clarify the functional association of DEGs, KEGG pathway enrichment analysis was performed on DEGs from the three comparisons **(Tables S7-S9)**. In the UD vs CK group, the significantly enriched pathways included Photosynthesis, Photosynthesis-antenna proteins, ABC transporters, Flavonoid biosynthesis, and Phenylpropanoid biosynthesis, etc. (Fig. 5A). In the OPPT vs UD group, the enriched pathways mainly involved Photosynthesis-antenna proteins, Photosynthesis, Plant-pathogen interaction, ABC transporters, Phenylpropanoid biosynthesis, and Flavonoid biosynthesis, etc. (Fig. 5B). In the OPPT vs CK group, the significantly enriched pathways included Photosynthesis, Photosynthesis-antenna proteins, ABC transporters, Phenylpropanoid biosynthesis, and Flavonoid biosynthesis, etc. (Fig. 5C). Among these pathways, 9 were significantly enriched in all three comparison groups: Photosynthesis, Photosynthesis - antenna proteins, ABC transporters, Carbon fixation in photosynthetic organisms, Biosynthesis of various plant secondary metabolites, Flavonoid biosynthesis, Phenylpropanoid biosynthesis, Cutin, suberine and wax biosynthesis, and alpha-Linolenic acid metabolism (Fig. 5).

3.5 Comparative Analysis of Untargeted Metabolome in Apple Fruits

To reveal the characteristics of the metabolic network of apple fruits regulated by OPPT, untargeted metabolomic analysis was performed on fruits from the CK group, UD group, and OPPT group, to systematically explore the composition and differential accumulation characteristics of metabolites in the three groups of samples. A total of 1709 metabolites were identified by untargeted metabolomic analysis **(Table S10)**, which were divided into 17 chemical categories based on their structural characteristics (Fig. 6A). Among them, Lipids and lipid-like molecules accounted for the highest proportion (26.86%), followed by Organic acids and derivatives (16.03%), Organic oxygen compounds (13.98%), Organoheterocyclic compounds

(13.46%), Phenylpropanoids and polyketides (12.93%), and Benzenoids (9.77%). The rest included Organic nitrogen compounds (2.05%), Alkaloids and derivatives (1.29%), and other categories (Fig. 6A). Principal component analysis (PCA) of metabolites showed that samples from the CK group, UD group, and OPPT group were clustered in different regions, with tight clustering of samples within groups and clear boundaries between groups. The first principal component (PC1) explained 43.78% of the metabolic variation, and the second principal component (PC2) explained 26.40% of the variation, with a cumulative variance contribution rate of 70.18%, which could effectively distinguish the differences in metabolite expression among the three groups of samples (Fig. 6B). Heat map visualization of metabolites showed that metabolites in all samples presented an obvious clustering pattern. The metabolite abundance patterns of samples within the same treatment group were highly similar, while there were significant differences between groups, reflecting the distinct metabolic profiles of the CK group, UD group, and OPPT group (Fig. 6C). To explore the dynamic change trend of metabolites in apple fruits under different treatment conditions, we performed K-means clustering analysis, and divided all metabolites into 4 subclasses according to the similarity of metabolite expression trends (Fig. 6D). Among them, subclass 3 had the highest number of metabolites (599). Subclass 1 (376 metabolites) had the highest metabolite abundance in the OPPT group and the lowest in the UD group; Subclass 2 (430 metabolites) had the highest metabolite abundance in the UD group, with similar abundance in the CK group and OPPT group; Subclass 3 (599 metabolites) had the highest metabolite abundance in the CK group, with similar abundance in the UD group and OPPT group; Subclass 4 (304 metabolites) had similar metabolite abundance in the UD group and OPPT group, which were significantly higher than that in the CK group.

To identify the key differentially accumulated metabolites (DAMs), orthogonal partial least squares discriminant analysis (OPLS-DA) was used to construct the model, and the variable importance in projection (VIP) score was calculated, which is a key indicator for identifying differential metabolites between samples. The R^2Y and Q^2 values of the model were both over 0.97, indicating good stability and strong predictive ability of the model, which could effectively distinguish samples between different groups **(Figure S1)**. DAMs were screened according to the criteria of VIP > 1.0, FC > 1.5 or FC < 0.667, and p-value < 0.05. Venn diagram analysis showed that there were no common DAMs among the three comparisons. There were 186 common DAMs between the UD vs CK group and the OPPT vs UD group, 180 common DAMs between the UD vs CK group and the OPPT vs CK group, and 122 common DAMs between the OPPT vs UD group and the OPPT vs CK group. There were 119 unique DAMs in the UD vs CK group, 85 unique DAMs in the OPPT vs UD group, and 89 unique DAMs in the OPPT vs CK group (Fig. 7A). The bar chart quantified the upregulated and downregulated DAMs in pairwise comparisons among the three groups of samples. A total of 485 DAMs were identified in the UD vs CK group, including 310 upregulated DAMs and 175 downregulated DAMs. A total of 393 DAMs were identified in the OPPT vs UD group, including 187 upregulated DAMs and 206 downregulated DAMs. A total of 391 DAMs were identified in the OPPT vs CK group, including 276 upregulated DAMs and 115 downregulated DAMs (Fig. 7B) **(Table S11)**. Compared with the CK group, most Lipids and lipid-like molecules showed an upregulated trend in the UD and OPPT treatment groups, with the most significant upregulation in the UD group. Phenylpropanoids and polyketides were significantly upregulated in the OPPT group, while they showed a certain degree of downregulation in the CK group and UD group as a whole, but the expression patterns of most specific metabolites were inconsistent. Organic acids and derivatives had the highest abundance in the OPPT group, were significantly downregulated in the CK group, and were at an intermediate level in the UD group. In addition, metabolites such as Organoheterocyclic compounds and Organosulfur compounds were significantly upregulated in the UD and OPPT treatment groups compared with the CK group, with the most significant upregulation in the UD group. Overall, compared with the CK group, the differential metabolites in the UD group and OPPT group showed an obvious upregulated trend, and the response of the OPPT group was in an intermediate state, with metabolite levels between those of the CK group and the UD group (Fig. 7C). KEGG pathway analysis revealed the key metabolic pathways of apple fruits with bitter pit in response to OPPT treatment. The top 20 enriched pathways for each comparison group were determined through enrichment and topological analysis to intuitively compare the differences in metabolic pathways among groups. Among them, the enriched pathways in the UD vs CK group involved Tryptophan metabolism, β-Alanine metabolism, Flavone and flavonol biosynthesis, Histidine metabolism, and Arginine biosynthesis, etc.; the enriched pathways in the OPPT vs UD group included Carotenoid biosynthesis, Tryptophan metabolism, Sesquiterpenoid and triterpenoid biosynthesis, Fatty acid biosynthesis, and Phosphonate and phosphinate metabolism, etc.; the OPPT vs CK group was enriched in Flavone and flavonol biosynthesis, Folate biosynthesis, Isoflavonoid biosynthesis, Steroid biosynthesis, and Flavonoid biosynthesis, etc. **(Figure S2A-C) (Tables S12-S14)**.

3.6 Integrated Analysis of Transcriptome and Metabolome in Apple Fruits

To reveal the molecular and metabolic mechanism of OPPT regulating the resistance of apple to bitter pit, integrated analysis of DEGs and DAMs was performed for the UD vs CK group, OPPT vs UD group, and OPPT vs CK group, respectively. KEGG co-enrichment analysis showed that a total of 36 pathways were co-enriched in the UD vs CK group, with the core pathways including Tryptophan metabolism, Carotenoid biosynthesis, and Plant hormone signal transduction, etc. The number of co-enriched pathways for DEGs and DAMs was significantly higher than that in the latter two groups (Fig. 8A). A total of 24 significant pathways were co-enriched in the OPPT vs UD group, with the core pathways being Tryptophan metabolism, Carotenoid biosynthesis, Linoleic acid metabolism, and Flavonoid biosynthesis, etc. (Fig. 8B). A total of 23 pathways were co-enriched in the OPPT vs CK group, with the core pathways including Flavonoid biosynthesis, Ubiquinone and other terpenoid–quinone biosynthesis, Cyanoamino acid metabolism, and Tryptophan metabolism, etc. (Fig. 8C). Among these pathways, 9 were enriched in both the OPPT vs UD group and the OPPT vs CK group: Tryptophan metabolism, Folate biosynthesis, Aminoacyl-tRNA biosynthesis, Steroid biosynthesis, Terpenoid backbone biosynthesis, Amino sugar and nucleotide sugar metabolism, Cysteine and methionine metabolism, 2-Oxocarboxylic acid metabolism, and Flavonoid biosynthesis (Fig. 8B-C). Among them, the Flavonoid biosynthesis pathway was selected for detailed characterization due to its significant activation and well-defined function in plant stress response. In the Flavonoid biosynthesis pathway of the OPPT vs UD group, three metabolites, namely (-)-Epigallocatechin, Liquiritigenin, and Naringenin chalcone, were found to be regulated by 9 genes, including those encoding key flavonoid synthesis enzymes CHS, FLS, HCT, CHI, and ANS **(Table S15)**. Correlation network analysis was performed on DEGs and DAMs in the Flavonoid biosynthesis pathway of the OPPT

vs UD group (| r|≥0.8, p-value ≤ 0.05). The results showed that two metabolites, (-)-Epigallocatechin and Naringenin chalcone, were significantly positively correlated with 8 regulatory genes and significantly negatively correlated with 1 regulatory gene, respectively **(**Fig. 8D**)**. Further analysis of the Flavonoid biosynthesis network in the OPPT vs CK group revealed that six metabolites, including Delphinidin, Naringenin, Dihydrokaempferol, Dihydroquercetin, (-)-Epigallocatechin, and Quercetin, were regulated by 14 genes, including those encoding key flavonoid synthesis enzymes CYP98A2, CHS, FLS, HCT, F3H, CHI, DFR, and ANS **(Table S16)**. Correlation network analysis was performed on DEGs and DAMs in the Flavonoid biosynthesis pathway of the OPPT vs CK group (| r|≥0.8, p-value ≤ 0.05). The results showed that five metabolites, including (-)-Epigallocatechin, Delphinidin, Naringenin, Dihydrokaempferol, and Quercetin, were significantly correlated with 13 regulatory genes, respectively **(Figure S3A)**. Notably, the Venn diagram of DEGs in the Flavonoid biosynthesis pathway between the OPPT vs UD group and the OPPT vs CK group showed that there were 9 DEGs in the OPPT vs UD group and 14 DEGs in the OPPT vs CK group, with 7 common DEGs between the two comparisons, including those encoding key flavonoid synthesis enzymes CHS, FLS, HCT, CHI, and ANS **(Figure S3B)**. These findings highlighted the co-expression characteristics of DEGs and DAMs in the Flavonoid biosynthesis pathway in apple fruits after OPPT treatment.

3.7 Analysis of Genes and Metabolites Involved in Flavonoid Biosynthesis in Apple Fruits

Integrated transcriptomic and metabolomic analysis indicated that OPPT treatment significantly regulated the Flavonoid biosynthesis pathway, which may be one of the key mechanisms for enhancing the resistance of apple fruits to bitter pit. To further explore this mechanism, we conducted a comprehensive study on the Flavonoid biosynthesis pathway in apple fruits after OPPT treatment. In this pathway, 9 differentially expressed genes (DEGs) were identified in the OPPT vs UD group, among which 8 genes were upregulated and 1 gene was downregulated, including those encoding key flavonoid synthesis enzymes CHS, FLS, HCT, CHI, and ANS. The expression changes of these genes were correlated with the accumulation of metabolites such as (-)-Epigallocatechin, Liquiritigenin, and Naringenin chalcone **(**Fig. 9A**)**, suggesting that OPPT treatment enhanced the antioxidant and stress resistance of fruits by activating the flavonoid synthesis pathway. In the OPPT vs CK group, 14 differentially expressed genes (DEGs) were identified, among which 1 gene was upregulated and 13 genes were downregulated, including those encoding key flavonoid synthesis enzymes CYP98A2, CHS, FLS, HCT, F3H, CHI, DFR, and ANS. These genes were correlated with metabolites such as Delphinidin, Naringenin, Dihydrokaempferol, Dihydroquercetin, (-)-Epigallocatechin, and Quercetin **(**Fig. 9A**)**. To further verify the reliability of the data, we selected 7 common DEGs (DVH24_000688, DVH24_006854, DVH24_024060, DVH24_031156, DVH24_022847, DVH24_037978, and DVH24_007939) shared by the OPPT vs UD and OPPT vs CK comparisons for RT-qPCR validation. The results showed that the expression trends of these genes were consistent with the transcriptome data **(**Fig. 9B**)**, and linear regression analysis showed a strong linear relationship between them ($R^2 > 0.95$), further confirming the reliability of the transcriptome results **(**Fig. 9C**)**. Notably, in the OPPT vs CK comparison, the genes related to the Flavonoid biosynthesis pathway showed an overall downregulated trend, indicating that OPPT treatment did not over-activate this pathway in healthy fruits, but significantly upregulated it under disease stress, reflecting its "stress response" characteristic. This further supports the key role of the Flavonoid biosynthesis pathway in the OPPT-mediated anti-bitter pit mechanism.

4. Discussion

4.1 Effect of OPPT on Apple Fruit Phenotype and Physiological Indicators

As a typical physiological disorder, the incidence of apple bitter pit is closely related to the disorder of fruit physiological metabolism, which severely restricts the high-quality development of the apple industry[4, 31, 32]. In this study, using the highly susceptible 'Qincui' apple as the material, we confirmed for the first time that OPPT treatment can significantly reduce the incidence of bitter pit at harvest, and its control efficacy far exceeds that of traditional measures such as calcium fertilization, providing a new approach for the green control of apple bitter pit. Fruit quality is the core indicator to measure the comprehensive benefit of control technology. OPPT treatment not only effectively controlled the disease, but also significantly improved the appearance and internal quality of fruits. Compared with the naturally diseased UD group, the single fruit weight, fruit firmness, and crispness were significantly increased in the OPPT group, the soluble sugar content was maintained at a high level, the titratable acid content was restored to the level of the healthy control group (CK), and the contents of non-enzymatic antioxidant substances such as vitamin C, total flavonoids, and total phenols were significantly higher than those in the CK group and UD group. These results are consistent with the dual effects of "disease control + quality improvement" exhibited by OPPT in the control of apple early defoliation disease[24, 25], confirming that its multi-component compound characteristics can achieve the synergistic gain of disease control and quality improvement.

At the physiological level, the occurrence of bitter pit is closely related to the imbalance of fruit mineral nutrition and metabolic disorder[7, 33, 34]. Although the soluble solids content in the UD group was significantly higher than that in the CK group, this may be a passive result of fruit dehydration and concentration under disease stress, rather than an active performance of quality improvement. The concomitant decrease in titratable acid and vitamin C contents further confirmed the occurrence of metabolic disorder. The OPPT group restored the normal accumulation of organic acids and vitamin C while maintaining fruit sweetness by regulating the balance of carbon and nitrogen metabolism, which is consistent with the quality improvement effect of carvacrol and chitosan when used alone[17, 20, 35]. It is speculated that their combination may synergistically regulate fruit respiratory metabolism and substance synthesis, and improve the accumulation pattern of nutritional components. In addition, the significant increase in total flavonoid and total phenol contents not only enhanced the antioxidant capacity of fruits, but also may reduce the epidermal

depression and browning related to bitter pit by improving the fruit epidermal structure and strengthening cell wall stability, which provides an important clue for the physiological mechanism of OPPT in controlling bitter pit.

4.2 Effect of OPPT on Apple Fruit Cell Structure and Calcium Distribution

Cell structural integrity and mineral element balance are important foundations for maintaining the normal physiological function of fruits and resisting diseases[26, 36–38]. The occurrence of bitter pit is often accompanied by the disorder of fruit cell structure and calcium metabolism imbalance. As an essential mineral element for plants, calcium plays a key role in maintaining cell wall stability, cell membrane permeability, and cell signal transduction[4]. In this study, through Safranin O-Fast Green staining and transmission electron microscopy observation, we found that the fruit cells in the UD group were loosely and disorderly arranged with structural rupture, and the morphology of organelles such as chloroplasts and mitochondria was abnormal with a reduced number. After OPPT treatment, the fruit cells were closely and neatly arranged, and the organelle morphology returned to normal, indicating that OPPT can effectively repair the cell structural damage caused by bitter pit. This result is consistent with the research conclusion that cell structural integrity directly affects fruit resistance[5, 8, 26, 39]. The repair of cell structure can reduce the invasion of harmful substances and the loss of cell contents, and enhance the resistance of fruits to diseases. SEM-EDS analysis showed that the Ca content was significantly reduced in the UD group compared with the CK group, while OPPT treatment significantly increased the fruit Ca content, restoring it to the level of healthy fruits. This finding revealed another important mechanism of OPPT in controlling bitter pit: improving calcium metabolism imbalance by supplementing calcium element. The occurrence of apple bitter pit has long been considered to be related to calcium deficiency. Insufficient calcium content will lead to reduced synthesis of calcium pectate in the cell wall, decreased cell wall strength, and easy cell rupture[4, 5, 40]. The stress-resistant nano ecological film in OPPT has a clear calcium supplementation function[16]. The calcium ions released by it can be absorbed by fruits, participate in cell wall synthesis and cell membrane stabilization, and regulate calcium-dependent signaling pathways to further enhance fruit stress resistance. In addition, the increased calcium content can also synergize with the antioxidant system to reduce ROS damage to cell structure, forming a dual protection of "structural repair + calcium balance", which is consistent with the previously reported mechanism of calcium in fruit disease defense [11].

4.3 Effect of OPPT on Apple Fruit Transcriptome and Metabolome

Transcriptomic and metabolomic analyses are two widely used high-throughput technologies in biological research. Integrated analysis of transcriptome and metabolome is the core method to elucidate the molecular mechanism of the occurrence and control of plant physiological diseases, which can reveal the disorder of molecular regulation caused by diseases and the core targets of control technologies from the two levels of gene expression and metabolite accumulation.

In this study, high-quality data were obtained from transcriptome sequencing, and there were significant differences in gene expression patterns among the three groups of samples. KEGG enrichment analysis showed that DEGs were mainly enriched in pathways such as Photosynthesis, ABC transporters, Flavonoid biosynthesis, and Phenylpropanoid biosynthesis, all of which are closely related to plant stress resistance and disease defense[41–45]. Untargeted metabolomic analysis identified 1709 metabolites, covering lipids, organic acids, phenylpropanoids, organoheterocyclic compounds, etc. KEGG enrichment analysis showed that DAMs in the UD vs CK group were mainly involved in pathways such as Tryptophan metabolism, β-Alanine metabolism, and Flavone and flavonol biosynthesis, reflecting the abnormal nitrogen metabolism and antioxidant metabolism in fruits during the occurrence of bitter pit. While DAMs in the OPPT vs UD group were enriched in pathways such as Carotenoid biosynthesis, Tryptophan metabolism, and Sesquiterpenoid and triterpenoid biosynthesis, indicating that OPPT repaired metabolic disorders by regulating these pathways. Notably, lipids and lipid-like molecules were significantly upregulated in the OPPT group, while lipid metabolism was disordered in the UD group. This is consistent with the function of lipids as important components of cell membranes to maintain membrane structural integrity[46, 47]. By repairing lipid metabolism, OPPT can enhance cell membrane stability, reduce oxidative damage and pathogen invasion.

Integrated analysis of transcriptome and metabolome further revealed the core pathways regulated by OPPT, among which Flavonoid biosynthesis, Tryptophan metabolism, Carotenoid biosynthesis and other pathways were co-enriched for DEGs and DAMs, indicating that these pathways are the key nodes regulated by OPPT. Among them, the Flavonoid biosynthesis pathway was selected for detailed characterization due to its significant activation and well-defined function in plant stress response. In this pathway, the synergistic upregulation of DEGs and DAMs confirmed that OPPT enhanced the synthesis and accumulation of flavonoids through the coordinated regulation of "genes-metabolites", which is consistent with the antioxidant and stress resistance functions of flavonoids[41, 48]. These results indicated that the regulation of OPPT on apple fruits is multi-pathway and multi-target, and the molecular control of bitter pit is achieved through the synergistic remodeling of transcriptome and metabolome.

4.4 Effect of OPPT on Flavonoid Biosynthesis in Apple Fruits

The Flavonoid biosynthesis pathway is one of the core pathways for plant stress resistance and defense. flavonoids (flavonols, anthocyanins, proanthocyanidins, etc.) have strong antioxidant activity, which can scavenge ROS, reinforce cell walls, regulate hormone signals, and play a key role in plant disease defense[49–51]. In this study, through integrated transcriptomic and metabolomic analysis, we found that the Flavonoid biosynthesis pathway is the core pathway regulated by OPPT, and it was significantly enriched in both the OPPT vs UD group and the OPPT vs CK group, confirming the key role of this pathway in the control of bitter pit by OPPT. In the OPPT vs UD group, 9 DEGs related to Flavonoid biosynthesis were identified, among which 8 were significantly upregulated, including key enzyme genes such as CHS (chalcone synthase), FLS (flavonol synthase), HCT (hydroxycinnamoyl transferase), CHI (chalcone isomerase), and ANS (anthocyanidin synthase). The upregulation of these genes directly promoted the

accumulation of flavonoid metabolites such as (-)-Epigallocatechin, Liquiritigenin, and Naringenin chalcone. CHS, as the key rate-limiting enzyme for flavonoid synthesis, its upregulated expression can accelerate the conversion of phenylpropane precursors to flavonoids[52–54]FLS and ANS regulate the synthesis of flavonols and anthocyanins, respectively, and these metabolites all have strong antioxidant activity, which can effectively scavenge ROS and reduce oxidative damage[55–57]. In the OPPT vs CK group, DEGs in the Flavonoid biosynthesis pathway were mainly downregulated, indicating that OPPT did not over-activate this pathway in healthy fruits, but specifically upregulated it under disease stress, reflecting the "stress response" regulatory characteristic and avoiding the waste of metabolic resources. Further correlation network analysis showed that (-)-Epigallocatechin and Naringenin chalcone were significantly positively correlated with 8 regulatory genes ($|r|\geq0.8$, $p \leq 0.05$) in the OPPT vs UD group, and 5 flavonoid metabolites were significantly correlated with 13 regulatory genes in the OPPT vs CK group, indicating that these genes and metabolites form a tight regulatory network to jointly mediate the control effect of OPPT. The qRT-PCR validation results showed that the expression trends of the 7 common DEGs were highly consistent with the transcriptome data ($R^2>0.95$), confirming the reliability of the transcriptome data and further verifying the regulatory role of key genes in the Flavonoid biosynthesis pathway. The mechanism of OPPT regulating the Flavonoid biosynthesis pathway may be related to the synergistic effect of its multiple components: as a plant-derived compound, carvacrol can induce the expression of key genes for flavonoid synthesis[17–19]; chitosan can activate plant defense signaling pathways and promote the synthesis of secondary metabolites[20–23]; the stress-resistant nano ecological film provides a suitable cellular environment for flavonoid synthesis through calcium supplementation and antioxidant effects [16]. The three act synergistically to jointly activate the Flavonoid biosynthesis pathway and improve fruit stress resistance. This is similar to the mechanism by which Glutathione (GSH) alleviates cadmium stress by regulating flavonoid synthesis[51], and also consistent with the research mechanism that cotton responds to tetrabromobisphenol A (TBBPA) stress by activating the Flavonoid biosynthesis pathway and promoting the accumulation of flavonoid metabolites such as naringenin to scavenge ROS and alleviate oxidative damage[58], indicating that the Flavonoid biosynthesis pathway is a conserved regulatory pathway for plants in response to adversity.

5. Conclusion

In this study, using the highly susceptible 'Qincui' apple as the research object, we systematically elucidated the mechanism of the three-in-one OPPT in controlling apple bitter pit from multiple dimensions of phenotype, physiology, cell, and molecule. The study found that OPPT treatment significantly reduced the incidence of apple bitter pit at harvest, while significantly improving fruit quality and ameliorating the physiological state of fruits. At the physiological level, OPPT alleviated oxidative stress by enhancing the activities of antioxidant enzymes such as SOD and CAT, increasing the contents of non-enzymatic antioxidant substances such as total flavonoids and total phenols, and reducing ROS accumulation and membrane lipid peroxidation damage. At the cellular level, OPPT repaired the cell structural disorder caused by bitter pit, increased the calcium content of fruits, and maintained the integrity of cell structure. At the molecular level, OPPT significantly reshaped the transcriptomic and metabolomic characteristics of fruits, and regulated multiple core pathways including Flavonoid biosynthesis, Tryptophan metabolism, and Carotenoid biosynthesis, among which the Flavonoid biosynthesis pathway was the key node regulated by OPPT. OPPT promoted the accumulation of flavonoid metabolites such as (-)-Epigallocatechin and Naringenin chalcone by upregulating the expression of key genes including CHS, FLS, HCT, CHI, and ANS, forming a synergistic regulatory network of "gene-metabolite-physiology-phenotype", and ultimately achieved effective control of apple bitter pit. This study revealed for the first time the molecular mechanism of OPPT in controlling apple bitter pit, filled the relevant research gap, provided a solid theoretical support for the optimization and promotion of OPPT, and also provided a novel strategy for the green control of apple physiological disorders, which is of great significance for promoting the sustainable development of the apple industry.

Declarations

Authors contribution

Zhu Li: Conceptualization, Methodology, Data curation, Formal analysis, Software, Supervision, Visualization, Funding acquisition, Writing – original draft, Writing – review & editing, Project administration. **Shikui Wang:** Writing – original draft, Supervision, Investigation, Data curation, Formal analysis. **Rongjing Cai:** Writing – original draft, Investigation, Resources, Data curation, Formal analysis. **Yingchun Huang:** Writing – original draft, Methodology, Investigation, Validation. **Bin Xia:** Writing – original draft, Investigation, Data curation, Validation. **Ling Mao:** Writing – original draft, Investigation, Data curation, Visualization. **Yanfei Song:** Writing – original draft, Investigation, Software, Data curation. **Tingmen Jiao:** Writing – original draft, Investigation, Software, Methodology. **Jiansong Qi** Writing – original draft, Investigation, Methodology, Data curation. **Yue Chen:** Conceptualization, Writing – original draft, Investigation, Data curation, Validation, Funding acquisition.

Funding

This work was supported by the Yunnan Fundamental Research Projects (202601AT070005), the Construction Project of the Engineering Research Center for Green Development of Zhaotong Apple Industry, Department of Education of Yunnan Province (Yun Jiao Fa [2024] No. 5), the Project of Scientific Research Start-up Funds for Doctoral Talents of Zhaotong University - Zhu Li (20240003), the Special Basic Cooperative Research Programs of Yunnan Provincial Undergraduate Universities' Association (202301BA070001-096), and the Yunnan Key Laboratory of Smart Villages and Agri-Cultural-Tourism Integration.

Declaration of competing interest

The authors declare that they have no known competing financial interests or personal relationships that could have appeared to influence the work reported in this paper.

Acknowledgments

We would like to acknowledge and thank those that contributed to our research and innovation discussions.

Appendix. A. Supplementary data

Supplementary data associated with this article can be found in the online version at XXXXX.

Data availability

The data that support the findings of this study are openly available: Transcriptomic raw data have been deposited in the NCBI Sequence Read Archive (SRA) under the BioProject accession number PRJNA1428194 (https://www.ncbi.nlm.nih.gov/bioproject/PRJNA1428194). Metabolomic raw data have been deposited to the EMBL-EBI MetaboLights database with the identifier MTBLS13937 (https://www.ebi.ac.uk/metabolights/MTBLS13937).

Ethics approval and consent to participate

This study involved only cultivated apple (*Malus domestica*) trees and did not involve human participants, human tissue, or experimental animals, so formal ethics committee approval was not required. **All field experiments and fruit sampling were conducted with the formal permission of the orchard landowners and farm management, in full compliance with local agricultural research guidelines and regulations.**

AI Use Statement

The author(s) declared that generative AI was not used in the creation of this manuscript.

References

1. Kithan-Lundquist R, Mcmillan HM, He SY, Sundin GW. Temporal fruit microbiome and immunity dynamics in postharvest apple (Malus x domestica). Hortic. Res. 2025; 12 (6), uhaf063. https://doi.org/10.1093/hr/uhaf063
2. Wood RM, Thewes FR, Reynaud M, Kittemann D, Sautter CK, Wuensche JN, et al. Apple fruit recovery from anoxia under controlled atmosphere storage. Food Chem. 2022; 371. https://doi.org/10.1016/j.foodchem.2021.131152
3. Lin Q, Chen J, Liu X, Wang B, Zhao Y, Liao L, et al. A metabolic perspective of selection for fruit quality related to apple domestication and improvement. Genome Biol. 2023; 24 (1), 95. https://doi.org/10.1186/s13059-023-02945-6
4. Torres E, Kalcsits L, Nieto LG. Is calcium deficiency the real cause of bitter pit? A review. Front. Plant Sci. 2024; 15, 14. https://doi.org/10.3389/fpls.2024.1383645
5. Islam MT, Liu J, Das PR, Singh A, Sherif SM. Rootstock effects on bitter pit incidence in 'Honeycrisp' apples are associated with changes in fruit's cell wall chemical properties. Front. Plant Sci. 2022; 13, 1034664. https://doi.org/10.3389/fpls.2022.1034664
6. Serban C, Kalcsits L, Deell J, Mattheis J. Responses of 'Honeycrisp' Apples to Short-term Controlled Atmosphere Storage Established During Temperature Conditioning. HortScience 2019. https://doi.org/10.21273/hortsci14182-19
7. Moggia C, Bravo MA, Baettig R, Valdés M, Romero-Bravo S, Zúñiga M, et al. Improving bitter pit prediction by the use of X-ray fluorescence (XRF): A new approach by multivariate classification. Front. Plant Sci. 2022; 13, 1033308. https://doi.org/10.3389/fpls.2022.1033308
8. Qiu L, Hu S, Wang Y, Qu H. Accumulation of abnormal amyloplasts in pulp cells induces bitter pit in malus domestica. Front. Plant Sci. 2021; 12, 738726. https://doi.org/10.3389/fpls.2021.738726
9. Xing Y, Zhang X, Feng Z, Ni W, Xie H, Guan Y, et al. Optimizing 'red Fuji' apple quality: Auxin-mediated calcium distribution via fruit-stalk in bagging practices. Food Chem. 2025; 463 (Pt 2), 141126. https://doi.org/10.1016/j.foodchem.2024.141126
10. Sun C, Zhang W, Qu H, Yan L, Li L, Zhao Y, et al. Comparative physiological and transcriptomic analysis reveal MdWRKY75 associated with sucrose accumulation in postharvest 'Honeycrisp' apples with bitter pit. BMC Plant Biol 2022; 22 (1), 71. https://doi.org/10.1186/s12870-022-03453-8
11. Bradleigh H, Tyerman SD, Burton RA, Matthew G. Fruit calcium: transport and physiology. Front. Plant Sci. 2016; 7, 569. https://doi.org/10.3389/fpls.2016.00569
12. Jemrić T, Fruk I, Fruk M, Radman S, Sinkovič L, Fruk G. Bitter pit in apples: pre- and postharvest factors: A review. Span. J. Agric. Res. 2016; 14 (4),e08 – e08. https://doi.org/10.5424/sjar/2016144-8491
13. Freitas STD, Amarante CVTD, Labavitch JM, Mitcham EJ. Cellular approach to understand bitter pit development in apple fruit. Postharvest Biol. Technol. 2010; 57 (1), 6-13. https://doi.org/10.1016/j.postharvbio.2010.02.006
14. De Freitas ST, Do Amarante CVT, Mitcham EJ. Mechanisms regulating apple cultivar susceptibility to bitter pit. Sci. Hortic. 2015; 186, 54-60. https://doi.org/10.1016/j.scienta.2015.01.039

15. Falchi R, D'Agostin E, Mattiello A, Coronica L, Spinelli F, Costa G, et al. ABA regulation of calcium-related genes and bitter pit in apple. Postharvest Biol. Technol. 2017; 132, 1-6. https://doi.org/10.1016/j.postharvbio.2017.05.017
16. Zheng YQ, Ma YS, Liu HY, Yang ZX, Ma YK, Guo HY, et al. Effects of different concentrations of Huadian stress-resistant ecological film on leaf, fruit traits, and cultivation effects of bag-free apples. Shaanxi J. Agric. Sci. 2024; 70(7), 22-28. https://doi.org/10.3969/j.issn.0488-5368.2024.07.005 (in Chinese)
17. Schorr RR, Ballesteros Garcia MJ, Petermann D, Moreira RR, Sales Maia BHLN, Marques FA, et al. Eugenol, Isoeugenol, Thymol, Carvacrol, and Ester Derivatives as an ecofriendly option to control glomerella leaf spot and bitter rot on apple. Plants (Basel) 2024; 13(22), 3196. https://doi.org/10.3390/plants13223196
18. Zhou D, Wei Y, Peng J, Tu S, Wang Z, Tu K. Carvacrol and eugenol inhibit postharvest soft rot disease by enhancing defense response in peaches during storage. J. Food Process. Preserv. 2019; 43 (9), e14086.1–e14086.11. https://doi.org/10.1111/jfpp.14086
19. Zhang L, Song R, Shi Z, Yuan S, Jiao L, Ma M, et al. Carvacrol effectively inhibits pseudomonas tolaasii in vitro and induces resistance to brown blotch disease in postharvest agaricus bisporus. Foods 2024; 13 (22), 3689. https://doi.org/10.3390/foods13223689
20. Riseh RS, Hassanisaadi M, Vatankhah M, Babaki SA, Barka EA. Chitosan as a potential natural compound to manage plant diseases. Int. J. Biol. Macromol. 2022; 220, 998-1009. https://doi.org/10.1016/j.ijbiomac.2022.08.109
21. Rojas-Pirela M, Carillo P, Lárez-Velásquez C, Romanazzi G. Effects of chitosan on plant growth under stress conditions: similarities with plant growth promoting bacteria. Front. Plant Sci. 2024; 15, 1423949. https://doi.org/10.3389/fpls.2024.1423949
22. Komarova T, Shipounova I, Kalinina N, Taliansky M. Application of chitosan and its derivatives against plant viruses. Polymers 2024; 16 (22), 3122. https://doi.org/10.3390/polym16223122
23. Degenring LM, Peter K, Poleatewich AM. Postharvest chitosan sprays reduce bitter rot and blue mold on apple fruit. Plant Dis. 2024; 109 (4), 909-920. https://doi.org/10.1094/pdis-07-24-1367-re
24. Zheng YQ, Liu SA, Feng HL, Ma YS, Sun GP. Effects of the "Three-in-One" green pest and disease control technology on leaf growth, fruit quality, and pesticide residues of bag-free apples. J. Fruit Res. 2024; 5(2), 51-55. https://doi.org/10.16010/j.cnki.14-1127/s.2024.02.01 (in Chinese)
25. Zheng YQ, Ma YS, Liu SA, Feng HL, Sun GP. Effects of green pest and disease control agents on cultivation effects of bag-free apples. Shaanxi J. Agric. Sci. 2024; 70(3), 90-96. https://doi.org/10.3969/j.issn.0488-5368.2024.03.017 (in Chinese)
26. Li Z, Zeng X, Chen Y, Shi H, Shao B, Gong R, et al. Regulation of nectarine flesh browning through pre-harvest application of chitosan coatings. Sci. Hortic. 2026; 356 (c), 114613. https://doi.org/10.1016/j.scienta.2026.114613
27. Ojo FM, Vendemiatti E, Júnior JL, Kumar-Mahto M, Benedito VA, Simes ARG. Determining trichome elemental composition in Solanum wild and domesticated species using SEM-EDS. Sci. Rep. 2025; 15 (1), 15292. https://doi.org/10.1038/s41598-025-87643-y
28. Dalvi VC, Rocha DI, Paula-Souza JD. Beyond leaf projections: the multifunctionality of leaf teeth in Violaceae. Sci. Nat. 2025; 112 (6), 77. https://doi.org/10.1007/s00114-025-02034-7
29. Liu GC, Li MF, Zhang Z, Han FL, Yan W, Liu YL, et al. Enhancement of grape heat tolerance through VvbZIP36-mediated quercetin production. Int. J. Biol. Macromol. 2025; 297, 139826. https://doi.org/10.1016/j.ijbiomac.2025.139826
30. Zhu L, Yang C, You Y, Liang W, Wang N, Ma F, Li C. Validation of reference genes for qRT-PCR analysis in peel and flesh of six apple cultivars (Malus domestica) at diverse stages of fruit development. Sci. Hortic. 2019; 244, 7. https://doi.org/10.1016/j.scienta.2018.09.033
31. Ferguson IB, Watkins CB. Bitter Pit in Apple Fruit. Wiley 1989. https://doi.org/10.1002/9781118060841.ch8
32. Sut-Lohmann M, Grimm M, Raab T, Heinrich M. Conventional vs. organic soil management practices in German apple orchards: Correlation between bitter pit disease incidence and nutrient status. EGU General Assembly, Vienna, Austria 2025. https://doi.org/10.5194/egusphere-egu24-16731
33. Zupan A, Mikulic-Petkovsek M, Cunja V, Stampar F, Veberic R. Comparison of phenolic composition of healthy apple tissues and tissues affected by bitter pit. J. Agric. Food Chem. 2013; 61 (49), 12066-12071. https://doi.org/10.1021/jf404087f
34. Xing Y, Zhu Z, Tian G, Du M, Cao H, Ge S. Physiological responses of apple to nitrogen fertilization regimes: roles of calcium metabolism in fruit quality and bitter pit development. Plants (Basel) 2026; 15 (12), 1820. https://doi.org/10.3390/plants15121820
35. Zhang X, Li K, Xing R, Liu S, Li P. Metabolite profiling of wheat seedlings induced by chitosan: revelation of the enhanced carbon and nitrogen metabolism. Front. Plant Sci. 2017; 8, 2017. https://doi.org/10.3389/fpls.2017.02017
36. Marzal A, Morales J, Primo-Capella A, Bermejo A, Martínez-Fuentes A, Quiñones A. Calcium reduces fruit abscission in persimmon by targeting cell wall integrity. Plants (Basel) 2025; 14 (22), 3482. https://doi.org/10.3390/plants14223482
37. Guo X, Li Q, Luo T, Han D, Zhu D, Wu Z. Postharvest calcium chloride treatment strengthens cell wall structure to maintain litchi fruit quality. Foods 2023; 12 (13). https://doi.org/10.3390/foods12132478
38. Jiang F, Gao S, Li M, Zhao Z, Yang C, Liu JH, et al. The multidimensional regulation roles and mechanisms of calcium in fruit quality. J. Integr. Plant Biol. 2026. https://doi.org/10.1111/jipb.70192
39. Shen X, Liu Y, Zeng Y, Zhao Y, Bao Y, Shao X, et al. Hydrogen sulfide attenuates chilling injury in loquat fruit by alleviating oxidative stress and maintaining cell membrane integrity. Food Chem. 2025; 463 (Pt 2), 141094. https://doi.org/10.1016/j.foodchem.2024.141094

40. Li Z, Chen Y, Kong BH, Song RT, Bai JN. Research progress on apple bitter pit: symptoms, mechanisms, and control. J. Fruit Sci. 2025; 43(4), 949-959. https://doi.org/10.13925/j.cnki.gsxb.20250203 (in Chinese)
41. Xu C, Wei L, Huang S, Yang C, Wang Y, Yuan H, et al. Drought resistance in qingke involves a reprogramming of the phenylpropanoid pathway and udp-glucosyltransferase regulation of abiotic stress tolerance targeting flavonoid biosynthesis. J. Agric. Food Chem. 2021; 69 (13), 3992-4005. https://doi.org/10.1021/acs.jafc.0c07810
42. Wu Y, Zhao H, Xiao M, Liu H, He H, Peng L, et al. A plant growth-promoting bacterium supports cadmium detoxification of rice by inducing phenylpropanoid and flavonoid biosynthesis. J. Hazard. Mater. 2025; 484. https://doi.org/10.1016/j.jhazmat.2024.136795
43. Li S, Chang L, Sun R, Dong J, Zhong C, Gao Y, et al. Combined transcriptomic and metabolomic analysis reveals a role for adenosine triphosphate-binding cassette transporters and cell wall remodeling in response to salt stress in strawberry. Front. Plant Sci. 2022; 13, 996765. https://doi.org/10.3389/fpls.2022.996765
44. Rajagopalan N, Lu Y, Burton IW, Monteil-Rivera F, Halasz A, Reimer E, Tweidt R, Brûlé-Babel A, Kutcher HR, You FM. A phenylpropanoid diglyceride associates with the leaf rust resistance Lr34res gene in wheat. Phytochemistry 2020; 178, 112456. https://doi.org/10.1016/j.phytochem.2020.112456
45. Shivhare R, Mishra P, Badola PK, Chauhan PS, Lata C. PgF3H gene enhances drought tolerance in transgenic Arabidopsis by regulating flavonoid biosynthesis and stress response. Plant Cell Rep. 2025; 44 (7), 150. https://doi.org/10.1007/s00299-025-03524-8
46. Wang L, Yang T, Pan Y, Shi L, Jin Y, Huang X. The metabolism of reactive oxygen species and their effects on lipid biosynthesis of microalgae. Int. J. Mol. Sci. 2023; 24 (13), 11041. https://doi.org/10.3390/ijms241311041
47. Liu X, Ren X, Fan Z, Mao P, Qian M, Qian T, et al. Metabolomics analysis reveals lipid metabolism disorders caused by triphenyltin via upregulation of PPARγ pathway. Ecotoxicol. Environ. Saf. 2025; 306, 119359. https://doi.org/10.1016/j.ecoenv.2025.119359
48. Li J, Yang J, Liang X, Zhan S, Bai Y, Ruan L. Melatonin-mediated regulation of antioxidant defense enhances the resistance of tea plants (Camellia sinensis L.) to lead-induced stress. Plants (Basel) 2025; 14 (10), 1417. https://doi.org/10.3390/plants14101417
49. Zhang J, Wang Y, Mao Z, Liu W, Ding L, Zhang X, et al. Transcription factor McWRKY71 induced by ozone stress regulates anthocyanin and proanthocyanidin biosynthesis in Malus crabapple. Ecotoxicol. Environ. Saf. 2022; 232, 113274. https://doi.org/10.1016/j.ecoenv.2022.113274
50. Jan R, Khan MA, Asaf S, Lubna, Park JR, Lee IJ, Kim KM. Flavonone 3-hydroxylase relieves bacterial leaf blight stress in rice via overaccumulation of antioxidant flavonoids and induction of defense genes and hormones. Int. J. Mol. Sci. 2021; 22 (11), 6152. https://doi.org/10.3390/ijms22116152
51. Fu Z, Yao Y, Haq MZU, Liu Y, Yang D, Yang H, et al. Glutathione's role in mitigating cadmium stress in Pogostemon cablin: Insights from combined transcriptomic and metabolomic approaches. J. Hazard. Mater. 2025; 491. https://doi.org/10.1016/j.jhazmat.2025.137921
52. Tong Y, Lyu Y, Xu S, Zhang L, Zhou J. Optimum chalcone synthase for flavonoid biosynthesis in microorganisms. Crit. Rev. Biotechnol. 2021; 41 (8), 1194-1208. https://doi.org/10.1080/07388551.2021.1922350
53. Waki T, Mameda R, Nakano T, Yamada S, Nakayama T. A conserved strategy of chalcone isomerase-like protein to rectify promiscuous chalcone synthase specificity. Nat. Commun. 2020; 11 (1), 870. https://doi.org/10.1038/s41467-020-14558-9
54. Lewis JA, Jacobo EP, Palmer N, Vermerris W, Sattler SE, Brozik JA, et al. Structural and interactional analysis of the flavonoid pathway proteins: chalcone synthase, chalcone isomerase and chalcone isomerase-like protein. Int. J. Mol. Sci. 2024; 25 (11), 27. https://doi.org/10.3390/ijms25115651
55. Fan L, Lin L, Zhang Y, Li S, Tang Z. Component characteristics and reactive oxygen species scavenging activity of anthocyanins from fruits of Lonicera caerulea L. Food Chem. 2023; 403, 134391. https://doi.org/10.1016/j.foodchem.2022.134391
56. Chapman JM, Muday GK. Flavonols modulate lateral root emergence by scavenging reactive oxygen species in Arabidopsis thaliana. J. Biol. Chem. 2020; 296, 100222. https://doi.org/10.1074/jbc.ra120.014543
57. Xu Z, Rothstein SJ. ROS-Induced anthocyanin production provides feedback protection by scavenging ROS and maintaining photosynthetic capacity in Arabidopsis. Plant Signal. Behav. 2018; 13(3), e145170. https://doi.org/10.1080/15592324.2018.1451708
58. Li X, Zhang Z, Huo W, Li J, Yang L, Ren Z, et al. Detoxification mechanisms of cotton in response to tetrabromobisphenol A stress revealed by integrated omics analysis. J. Hazard. Mater. 2026; 501, 140954. https://doi.org/10.1016/j.jhazmat.2025.140954

Figures

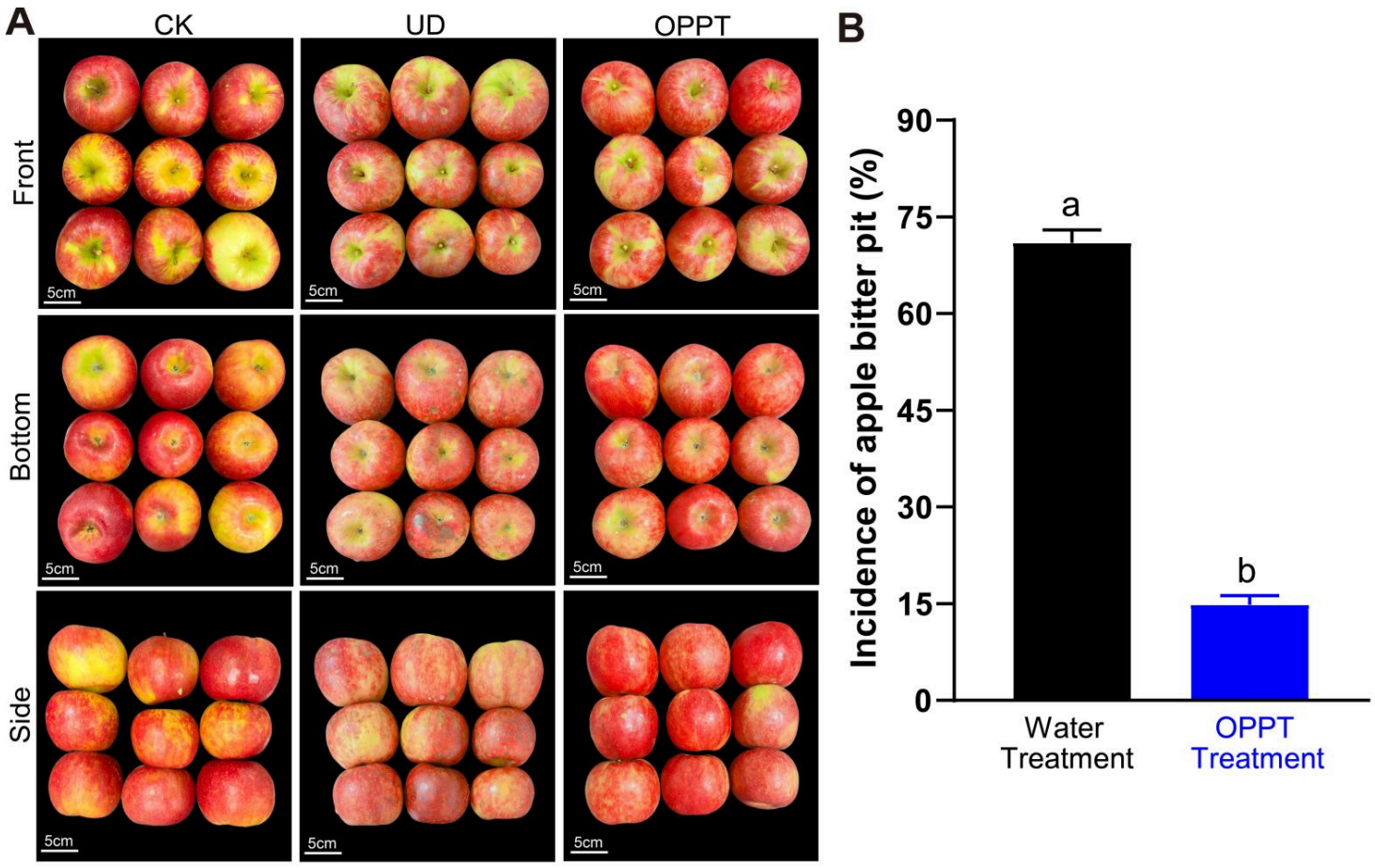


Figure 1

Incidence of apple bitter pit at harvest. (A) Phenotype of bitter pit in 'Qincui' apples at harvest. (B) Incidence rate of bitter pit in 'Qincui' apples at harvest. CK group: untreated healthy control group; UD group: untreated diseased group; OPPT group: OPPT-treated healthy group. (n=300), different lowercase letters indicate significant differences between groups (p<0.05).

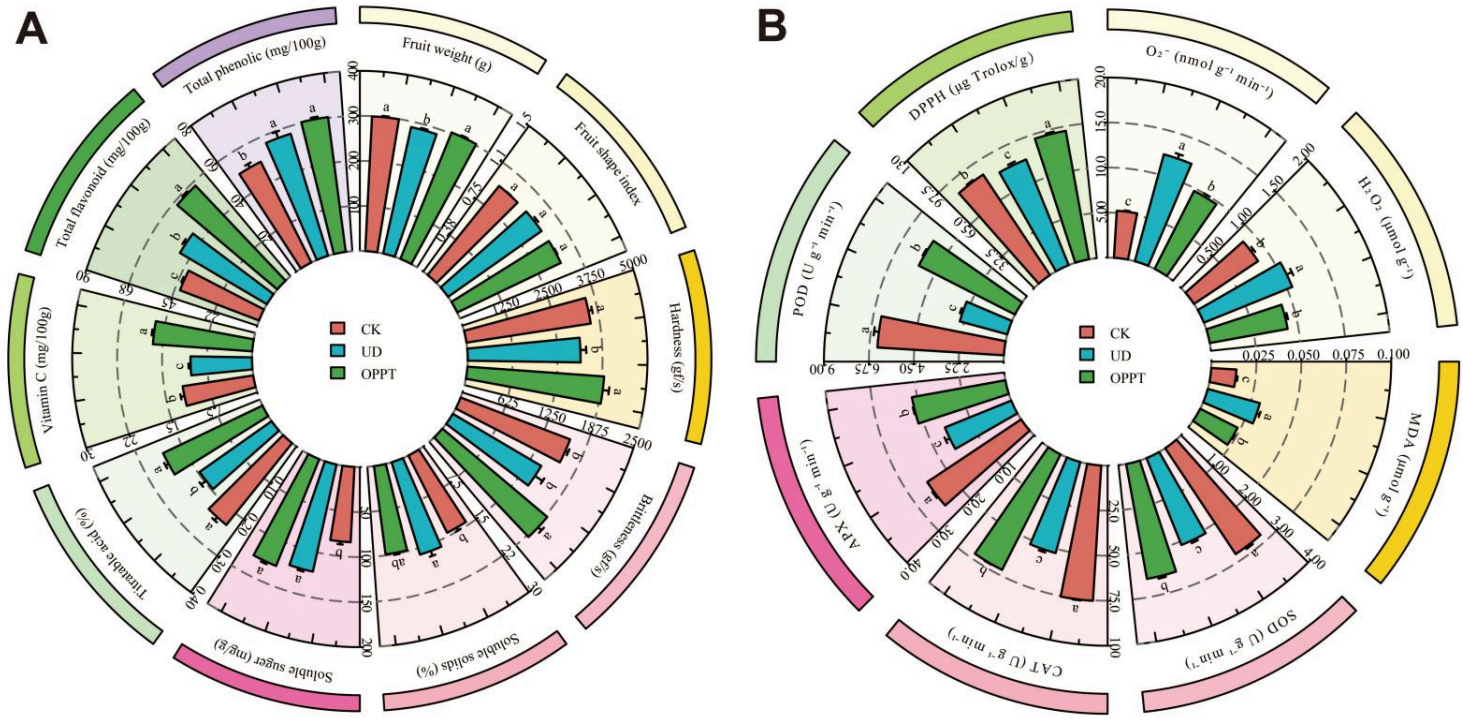


Figure 2

Analysis of apple fruit quality, oxidative damage, and antioxidant enzymes. (A) Apple fruit quality. Vitamin C: reduced ascorbic acid. (B) Analysis of oxidative damage and antioxidant enzymes in apple fruits. MDA: malondialdehyde; SOD: superoxide dismutase; CAT: catalase; APX: ascorbate peroxidase; POD: peroxidase; DPPH: 1,1-Diphenyl-2-picrylhydrazyl radical. CK group: untreated healthy control group; UD group: untreated diseased group; OPPT group: OPPT-treated healthy group. (n=3), different lowercase letters indicate significant differences between groups (p<0.05).

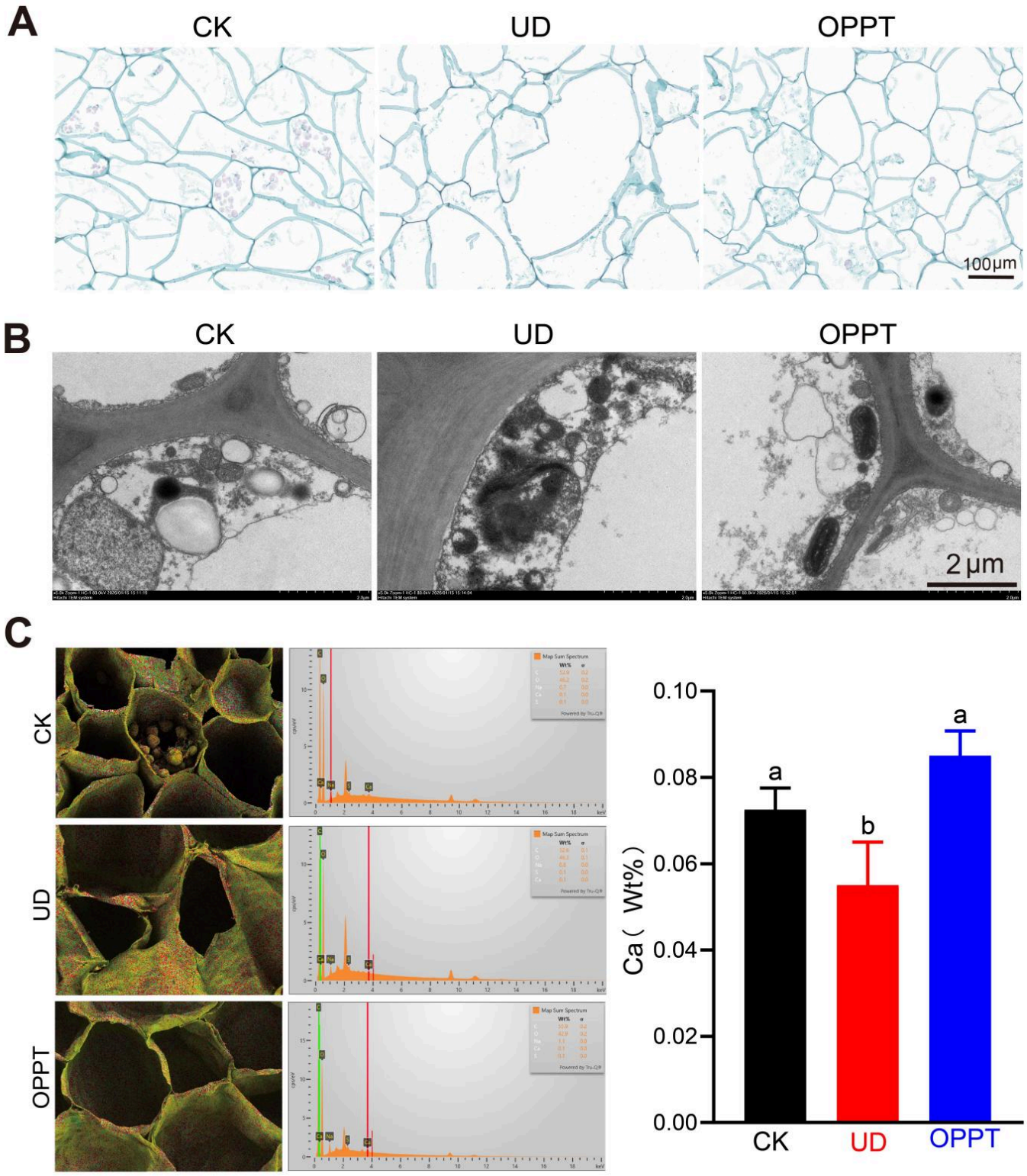


Figure 3

Cytological and Ca element analysis of apple fruits. (A) Safranin O-Fast Green staining. (B) Transmission electron microscopy. (C) Scanning electron microscopy with energy dispersive spectroscopy (SEM-EDS) and quantitative analysis of Ca element. CK group: untreated healthy control group; UD group: untreated diseased group; OPPT group: OPPT-treated healthy group. (n=3), different lowercase letters indicate significant differences between groups (p<0.05).

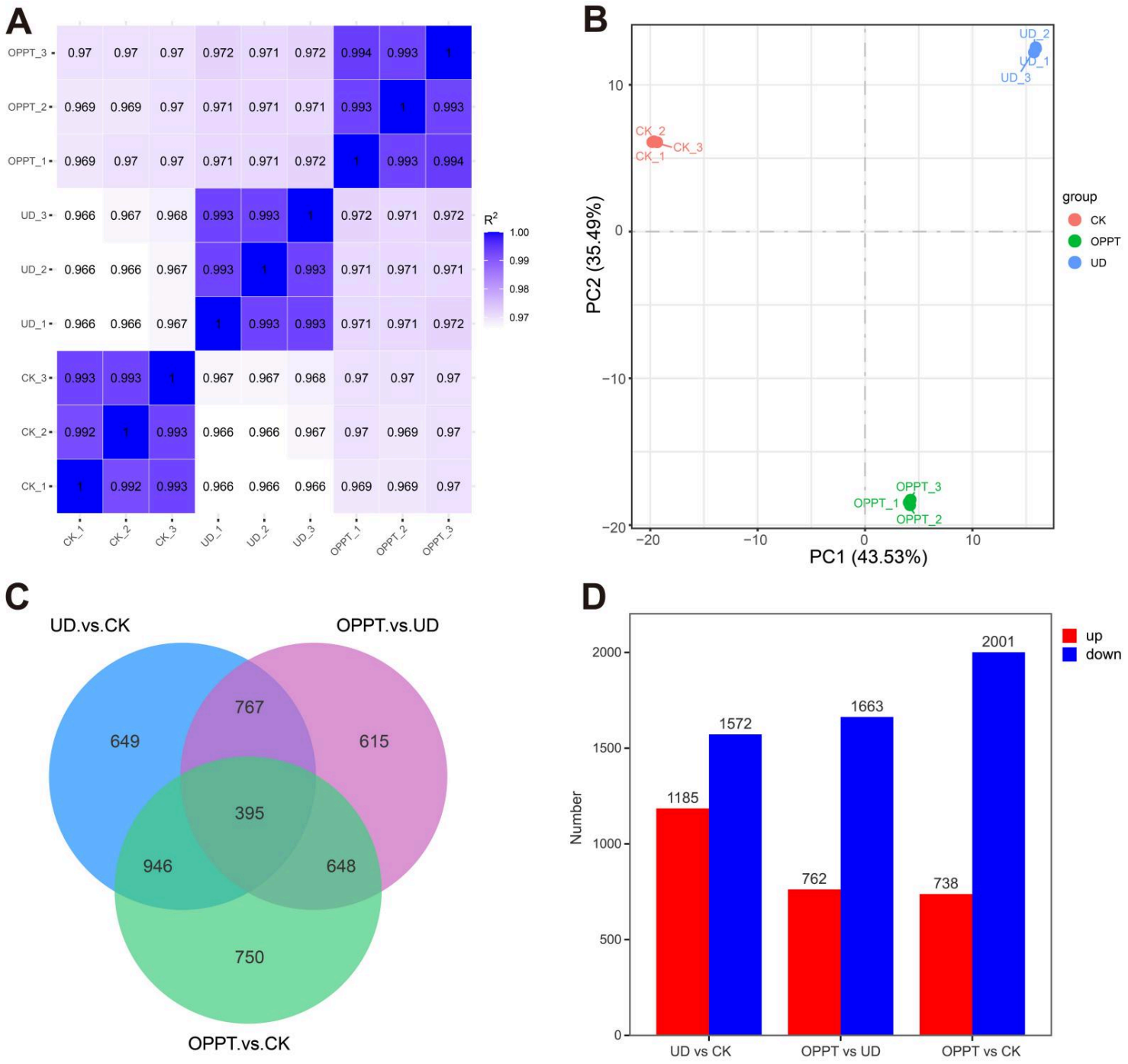


Figure 4

Transcriptomic analysis of apple fruits. (A) Correlation analysis of the three groups of samples. (B) Principal component analysis (PCA) of the three groups of samples. (C) Venn diagram analysis of DEGs in the three comparison groups (UD vs CK, OPPT vs UD, and OPPT vs CK). (D) Bar chart of upregulated and downregulated DEGs in the three comparison groups (UD vs CK, OPPT vs UD, and OPPT vs CK). CK group: untreated healthy control group; UD group: untreated diseased group; OPPT group: OPPT-treated healthy group. (n=3).

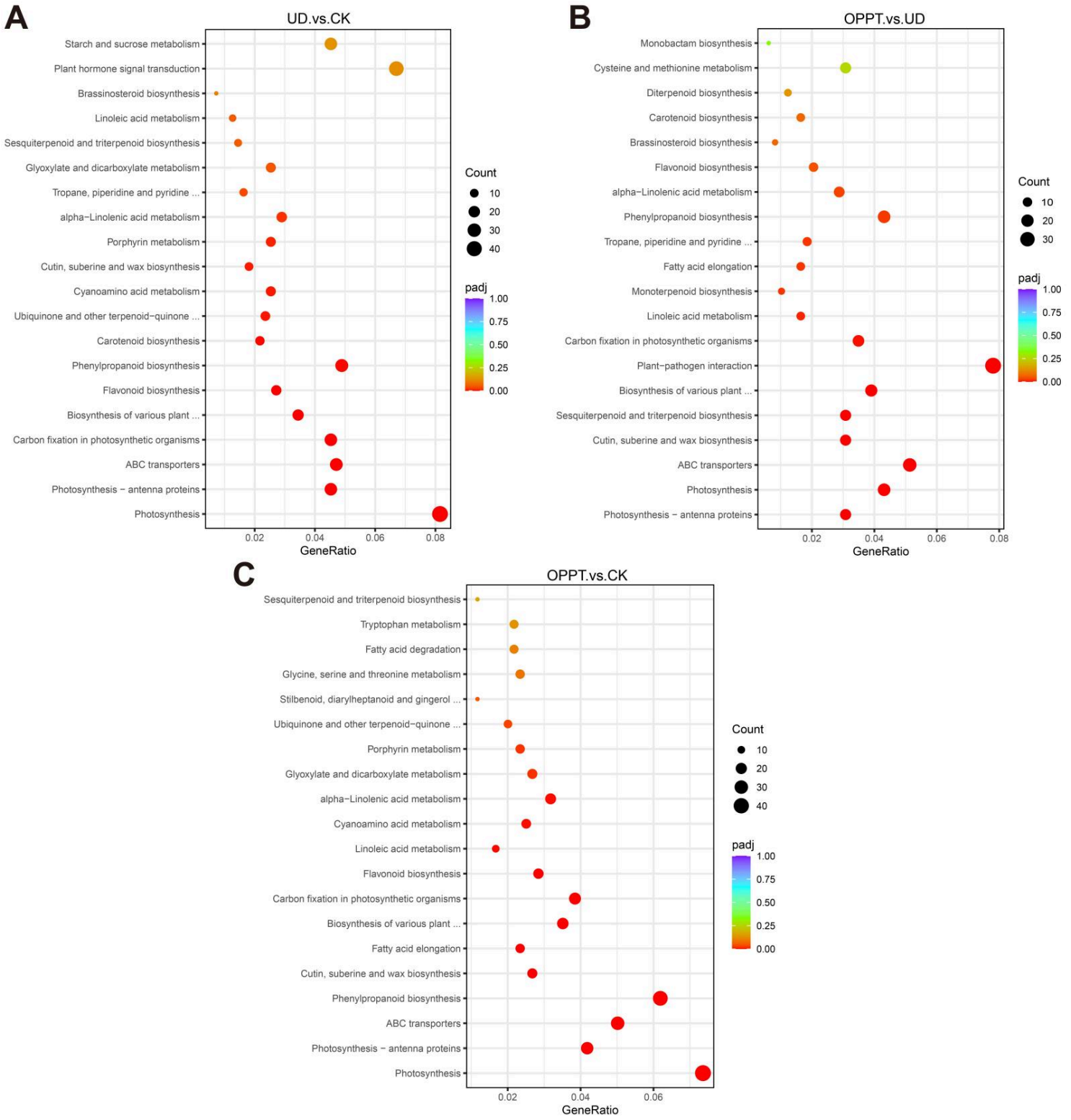


Figure 5

KEGG pathway analysis of differentially expressed genes (DEGs). (A) KEGG analysis of DEGs in the UD vs CK group. (B) KEGG analysis of DEGs in the OPPT vs UD group. (C) KEGG analysis of DEGs in the OPPT vs CK group. CK group: untreated healthy control group; UD group: untreated diseased group; OPPT group: OPPT-treated healthy group. (n=3).

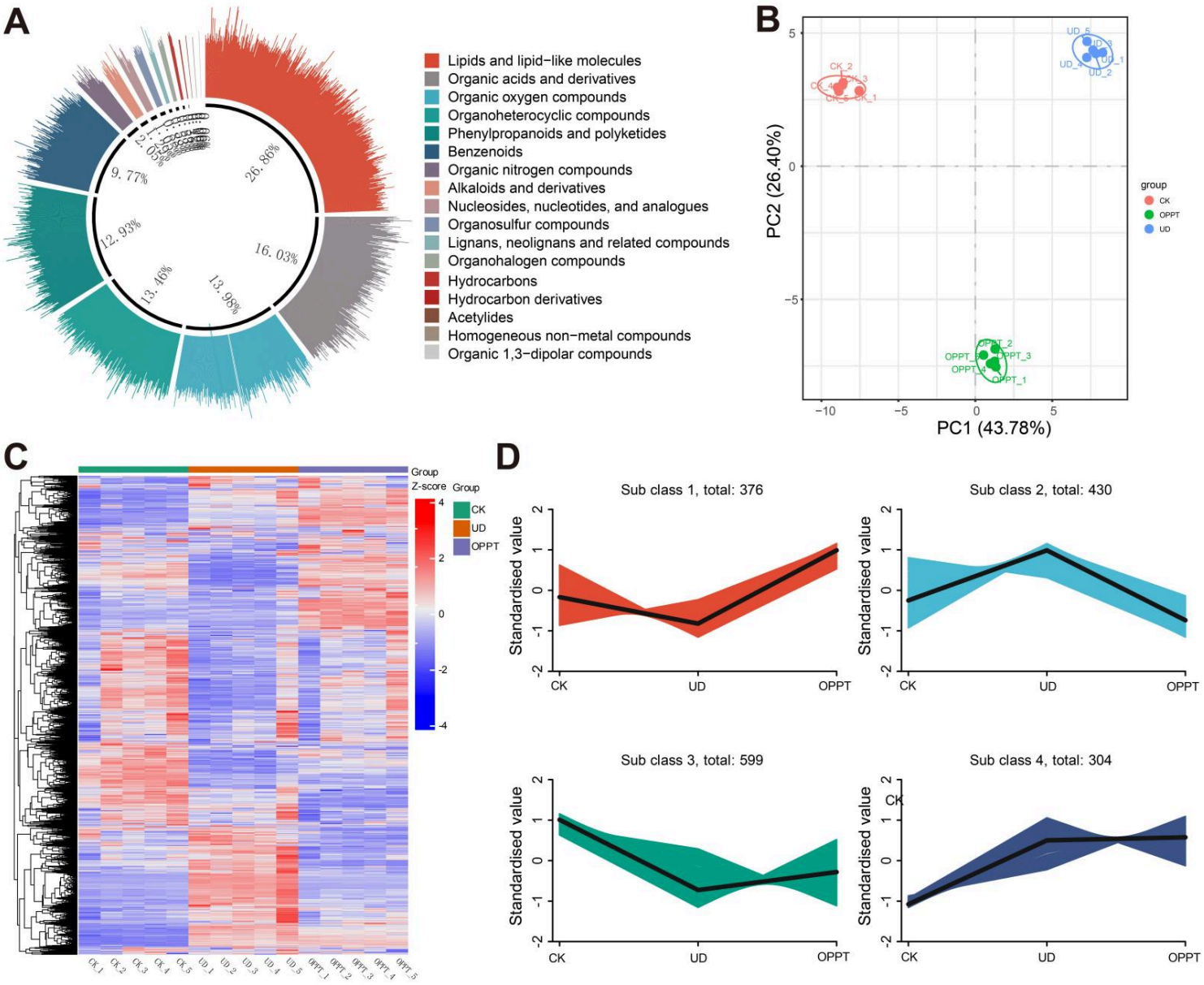


Figure 6

Metabolomic analysis of apple fruits. (A) Chemical structure classification and statistical analysis of metabolites. (B) Principal component analysis of metabolites. (C) Heat map visualization of metabolites, red indicates high-abundance metabolites, and blue indicates low-abundance metabolites. (D) K-means clustering analysis (metabolites were divided into 4 subclasses). CK group: untreated healthy control group; UD group: untreated diseased group; OPPT group: OPPT-treated healthy group. (n=5).

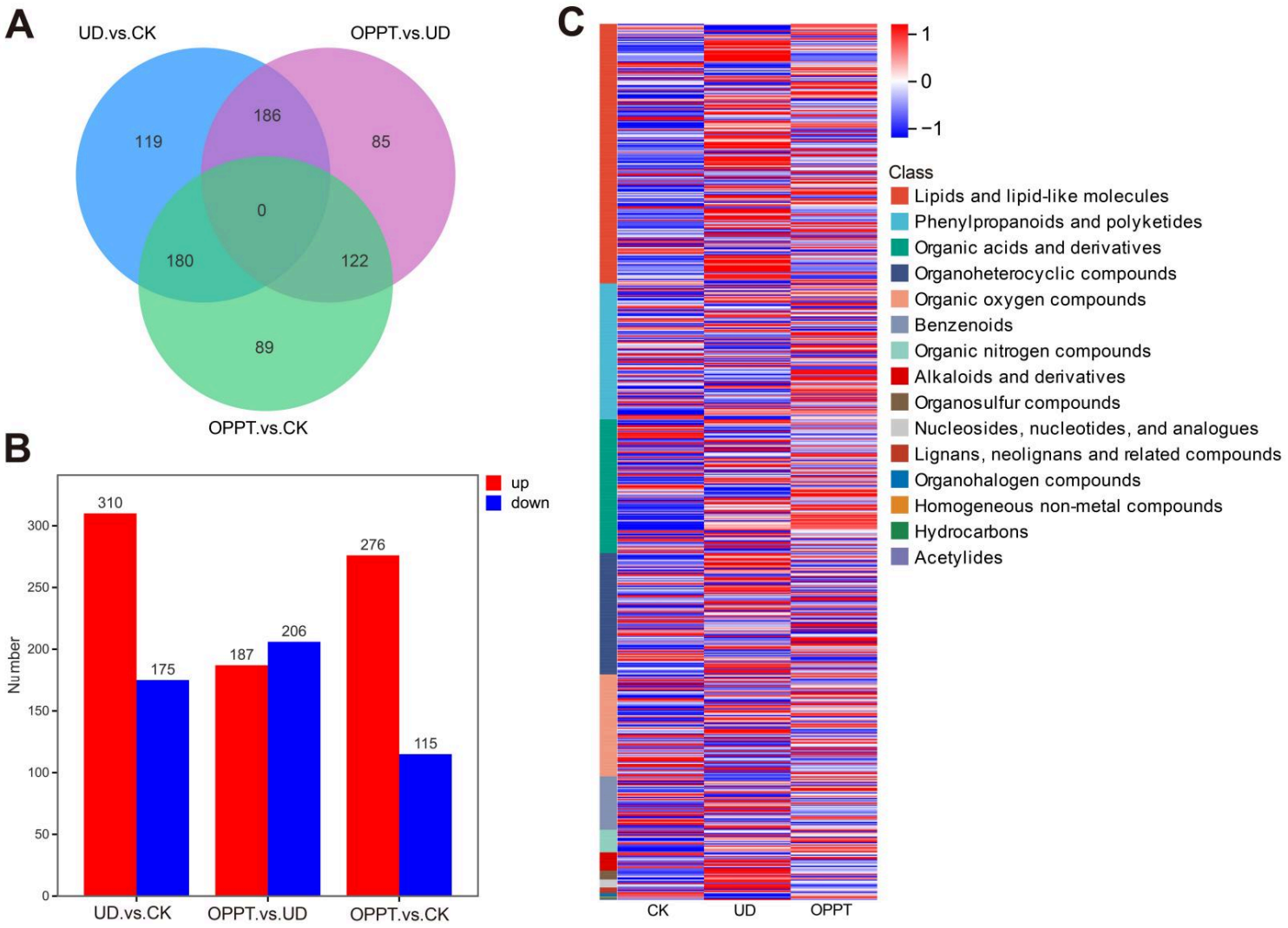


Figure 7

Differential analysis of the metabolome in apple fruits. (A) Venn diagram analysis of DAMs in the three comparison groups (UD vs CK, OPPT vs UD, and OPPT vs CK). (B) Bar chart quantifying the differential accumulation of DAMs (upregulated and downregulated) in the three comparison groups (UD vs CK, OPPT vs UD, and OPPT vs CK). (C) Heat map visualization of DAMs, red indicates high-abundance metabolites, and blue indicates low-abundance metabolites. CK group: untreated healthy control group; UD group: untreated diseased group; OPPT group: OPPT-treated healthy group. (n=5).

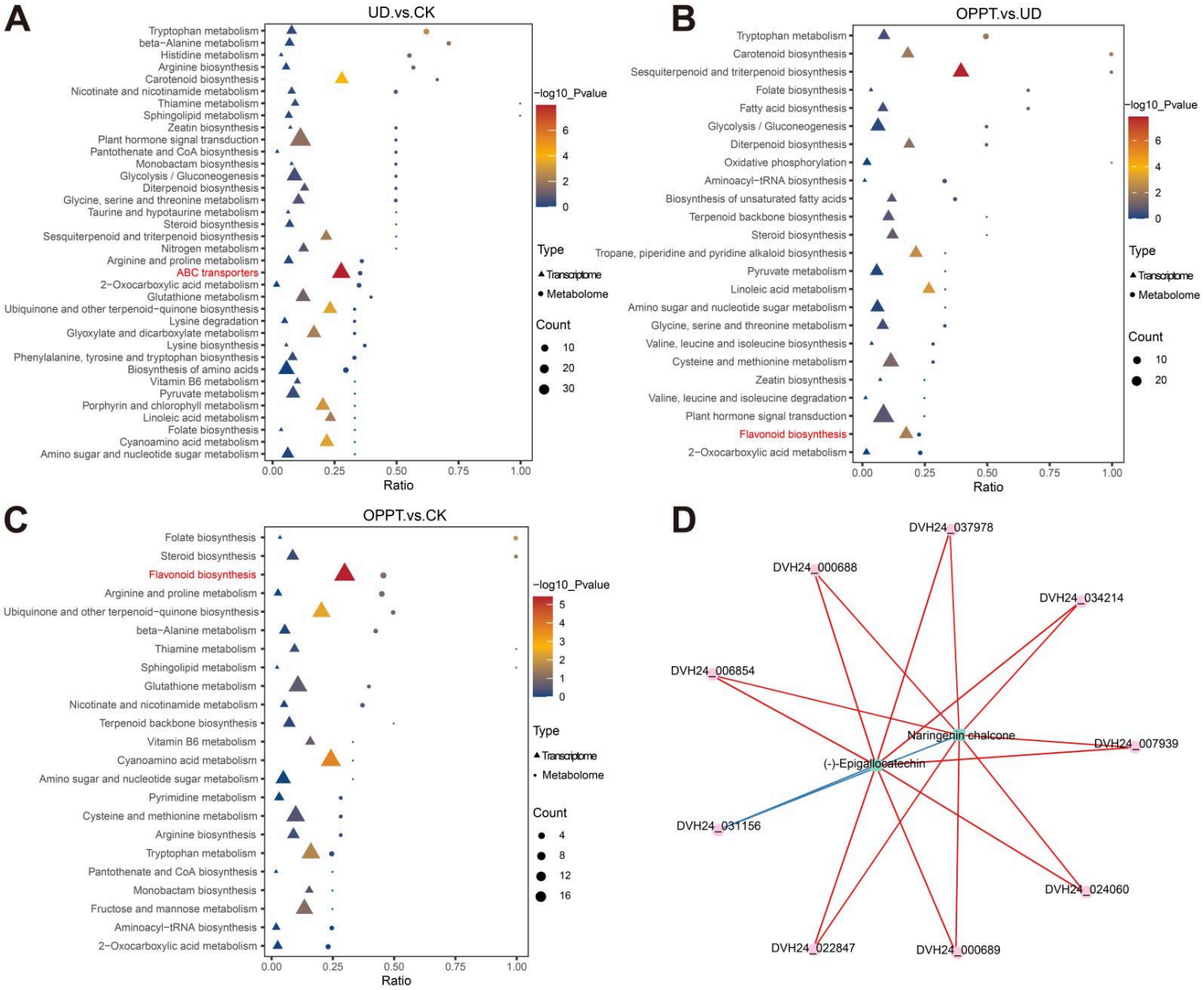


Figure 8

Network analysis of DEGs and DAMs in apple fruits. (A) KEGG co-enrichment analysis of DEGs and DAMs in the UD vs CK group. (B) KEGG co-enrichment analysis of DEGs and DAMs in the OPPT vs UD group. (C) KEGG co-enrichment analysis of DEGs and DAMs in the OPPT vs CK group. (D) Correlation network analysis of DEGs and DAMs in the Flavonoid biosynthesis pathway of the OPPT vs UD group. Red squares represent differential genes, blue circles represent differential metabolites, red lines represent positive correlations, and blue lines represent negative correlations. CK group: untreated healthy control group; UD group: untreated diseased group; OPPT group: OPPT-treated healthy group.

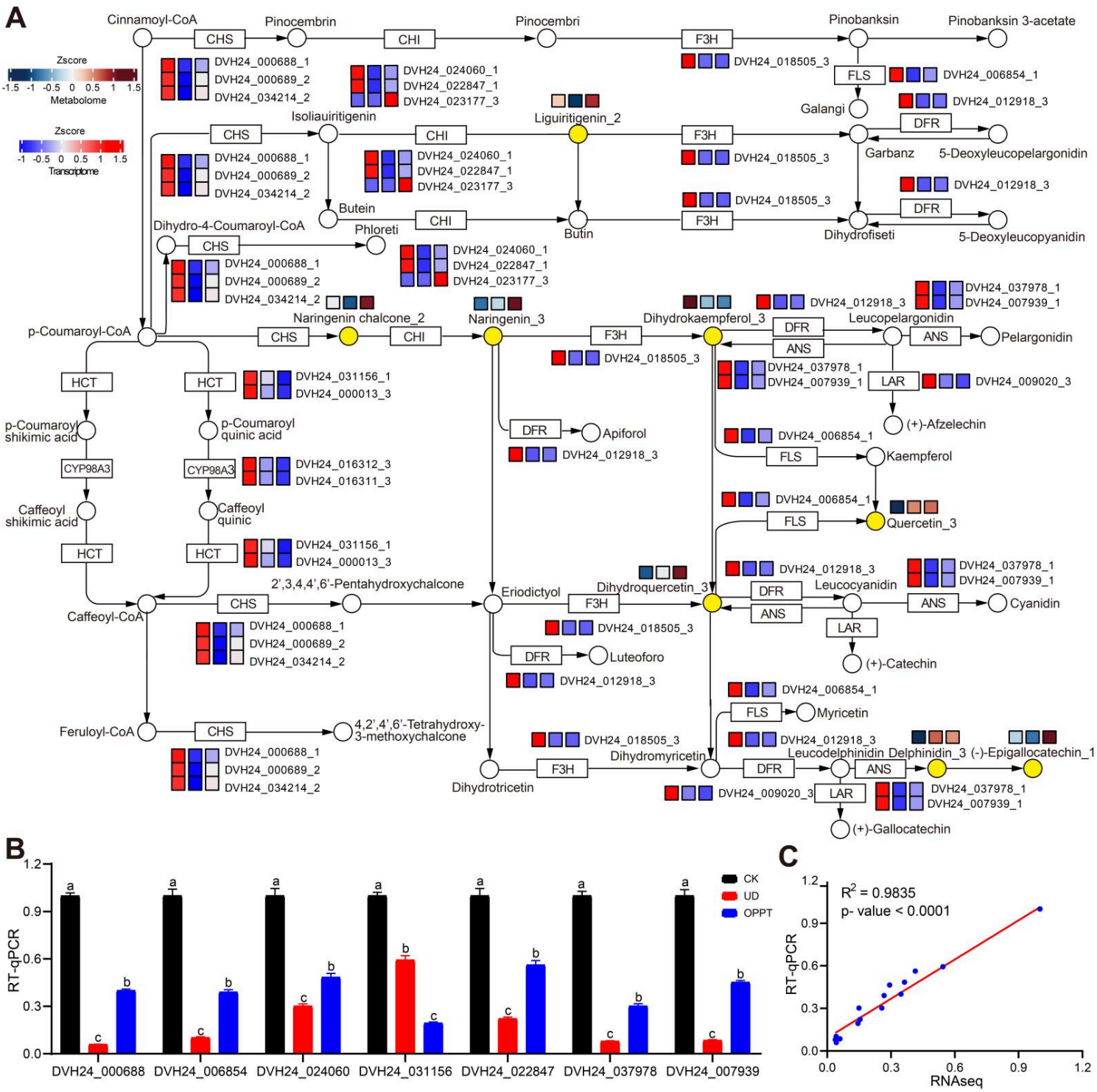


Figure 9

Effect of OPPT treatment on genes and metabolites involved in Flavonoid biosynthesis in apple fruits. (A) Profile of DEGs and DAMs in the Flavonoid biosynthesis pathway in apple fruits. CHS: chalcone synthase; FLS: flavonol synthase; HCT: hydroxycinnamoyl transferase; CHI: Chalcone isomerase; ANS: anthocyanidin synthase (_1: Common to OPPT vs UD and OPPT vs CK, _2: Unique to OPPT vs UD, _3: Unique to OPPT vs CK). (B) RT-qPCR validation of transcriptome data for flavonoid metabolism-related genes in apple fruits. (C) Linear regression analysis of relative expression levels between RT-qPCR and RNA-seq ($R^2 > 0.95$, $p < 0.0001$). CK group: untreated healthy control group; UD group: untreated diseased group; OPPT group: OPPT-treated healthy group. (n=3), different lowercase letters indicate significant differences between groups ($p<0.05$).

Supplementary Files

This is a list of supplementary files associated with this preprint. Click to download.

- SupplementaryTable.xlsx
- Highlights.docx
- SupplementaryFigure.docx
- GraphicalAbstract.docx